AD_____

Award Number:

W81XWH-09-2-0022

TITLE:
Development of Novel Vaccines and Therapeutics Using Plant-Based Expression Systems

PRINCIPAL INVESTIGATOR:

Keith R. Davis, Ph.D.

CONTRACTING ORGANIZATION:

Owensboro Medical Health System, Inc.
Owensboro, KY 42303

REPORT DATE:

April 2010

TYPE OF REPORT:

Annual Report

PREPARED FOR: U.S. Army Medical Research and Materiel Command
Fort Detrick, Maryland 21702-5012

DISTRIBUTION STATEMENT:

☑ Approved for public release; distribution unlimited

REPORT DOCUMENTATION PAGE

Form Approved
OMB No. 0704-0188

1. REPORT DATE *(DD-MM-YYYY)*	2. REPORT TYPE	3. DATES COVERED *(From - To)*
01-04-2010	Annual	15 Mar 2009 - 14 Mar 2010

4. TITLE AND SUBTITLE
Development of Novel Vaccines and Therapeutics Using Plant-Based Expression Systems

5a. CONTRACT NUMBER
3

5b. GRANT NUMBER
W81XWH-09-2-0022

5c. PROGRAM ELEMENT NUMBER

6. AUTHOR(S)
Keith R. Davis, Ph.D.

5d. PROJECT NUMBER

5e. TASK NUMBER

5f. WORK UNIT NUMBER

7. PERFORMING ORGANIZATION NAME(S) AND ADDRESS(ES)
Owensboro Medical Health
Systems, Inc.

Owensboro, KY 42303-3258

8. PERFORMING ORGANIZATION REPORT NUMBER

9. SPONSORING / MONITORING AGENCY NAME(S) AND ADDRESS(ES)
U.S. Army Medical Research and
and Material command
Fort Detrick, Maryland
21702-5012

10. SPONSOR/MONITOR'S ACRONYM(S)

11. SPONSOR/MONITOR'S REPORT NUMBER(S)

12. DISTRIBUTION / AVAILABILITY STATEMENT
Approved for public release; distribution unlimited

13. SUPPLEMENTARY NOTES

14. ABSTRACT

The primary focus of this award is to support the development of the Owensboro Cancer Research Program. Projects include the development of the soybean peptide lunasin as a chemoprevention agent; the development of the antiviral proteins griffithsin and actinohivin; and functional analysis of genes important for embryonic stem cell development and differentiation into neuronal stem cells. The development of lunasin as a chemoprevention agent and/or therapeutic is now at the point where preclinical studies can be started as a prelude to potential clinical trials. The development of griffithsin has been significantly advanced, particularly with respect to indications other than HIV. It is anticipated that preclinical studies of griffithsin will be largely completed during the next two years. It is anticipated that the utility of actinohivin as an antiviral microbicide will be clearly delineated over the next year. Although the stem cell is the most basic project being supported, it has significant relevance to developing methods for controlling the differentiation of neuronal stem cells from embryonic stem cells. Specific product oriented research will be initiated when a clear target emerges from this preliminary work.

15. SUBJECT TERMS
Plant-made pharmaceuticals, chemoprevention, antiviral proteins, calcium signaling

16. SECURITY CLASSIFICATION OF:			17. LIMITATION OF ABSTRACT	18. NUMBER OF PAGES	19a. NAME OF RESPONSIBLE PERSON
a. REPORT	b. ABSTRACT	c. THIS PAGE			USAMRMC
U	U	U	UU	71	19b. TELEPHONE NUMBER *(include area code)*

Table of Contents

	Page
Introduction……..	**4**
Body……..	**4-15**
Key Research Accomplishments……..	**15-16**
Reportable Outcomes……	**16-22**
Conclusion……	**22**
Appendices……	**22-71**

INTRODUCTION

The primary focus of this award is to support the development of the Owensboro Cancer Research Program (OCRP). The major goal of the OCRP is to become the premier academic research enterprise in the world that combines the field of plant-made pharmaceuticals with the prevention and treatment of cancer and infectious disease. The OCRP currently includes four principal investigators who are full-time faculty members in the University of Louisville School of Medicine. The award funds are being utilized to support specific research projects within each faculty member's laboratory. These research projects include the development of the soybean peptide lunasin as a chemoprevention agent and cancer therapeutic; the development of the antiviral proteins griffithsin and actinohivin; and functional analysis of specific genes important for embryonic stem cell development and differentiation into neuronal stem cells. In addition to specific research outcomes derived from these projects, other project milestones include specific objectives that represent the successful establishment of this new program. These objectives include the recruitment of additional faculty; the establishment of a solid base of competitive grants; the development of novel therapeutics; and the establishment of research collaborations with other academic laboratories and industry partners.

BODY

Research Accomplishments

Faculty members at the OCRP have diverse research interests that are linked by the use of plant-based expression systems for translational research. The funds from this award are being used to expand these research programs and to support new pilot projects. The specific research projects that have been supported by this award to date are in the areas of developing a new cancer therapeutic, several projects on the development of antiviral proteins for the prevention and treatment of major viral diseases, and the identification of key regulatory genes that affect the differentiation of embryonic stem cells into neuronal stems cells. The results obtained during the first of year of funding are summarized in the following sections.

Development of Lunasin as a Chemoprevention Agent (Dr. Keith R. Davis)

Lunasin is a small peptide consisting of 43 amino acids with a C-terminal end of nine consecutive aspartic acid residues. Lunasin was originally isolated from soybean but has been found in a variety of plant species at relatively low levels. Initial studies demonstrated that lunasin can prevent the transformation of mammalian cells by chemical carcinogens or viral oncogenes; however, lunasin has little effect on normal or established cancer cell lines. This chemopreventive effect on cells undergoing a transformation event is thought to be mediated by the disruption of mitosis and induction of apoptosis. More recent studies suggest that lunasin binds to deacetylated core histones and exerts its effects via an epigenetic mechanism that disrupts the normal dynamics of histone acetylation-deacetylation. Although the potential cancer-

chemopreventive activity has been known for almost a decade, little progress has been made to demonstrate clinical relevance. Attempts to express lunasin in E. coli, yeast, and animal cells have been unsuccessful, thus limiting studies to quantities of lunasin that can be synthesized or purified from natural sources. The major goals of this project are to develop robust methods for the purification of native lunasin from soybean, develop methods for producing modified recombinant forms of lunasin, and the development of lunasin as a chemoprevention agent and/or cancer therapeutic. Significant progress has been made in all three of these research areas.

Purification of Lunasin from Soybean

Most of our effort has been directed towards this critical goal and it has now been successfully completed. We have developed a robust purification method based on using white flake, (the crude protein preparation remaining after oil removal and extraction with hexane) as the starting material. An overview of this method is shown in Figure 1. The major steps of the method are as follows. White flake is suspended in 12 volumes of PBS (58.5 mM Na2HPO4, 17 mM $NaH2PO_4$, 68.4 mM NaCl, 20 mM ascorbic acid, 10 mM sodium metabisulfite) and stirred for two hours at room temperature. The resulting extract is clarified using a filter press to remove all the particulates. The clarified extract is subjected to anion-exchange chromatography on a Q Sepharose FF column (GE Healthcare) using a linear NaCl gradient up to 1 M NaCl. Free lunasin and the lunasin complex elute from the column at ~ 0.35 M NaCl. The lunasin containing fractions are pooled and subjected to ultrafiltration with a 30 kD MWCO membrane. Lunasin is present in the permeate. The permeate is concentrated and desalted by UF/DF. The concentrated permeate is brought to 2 mM DTT to reduce the lunasin complex and generate free lunasin. The reduced permeate is brought to 1 M ammonium sulfate and subjected to hydrophobic chromatography using a Butyl FF column (GE Healthcare). Lunasin passes through the column and is collected in the flow through. The flow through is then subjected to reverse phase chromatography using a Resource 15 RPC column (GE Healthcare). Lunasin elutes from the column at 15% n-propanol. The lunasin-containing fractions are pooled and subjected to UF/DF to concentrate and exchange the elution buffer with PBS. The resulting purified lunasin is filter-sterilized, aliquoted, and stored at -20

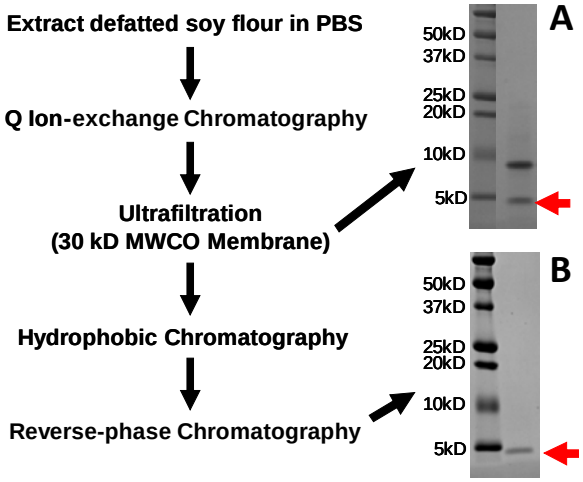

Figure 1. Summary of lunasin purification method. The major steps are shown in the flow diagram. Coomassie-stained denaturing SDS-PAGE gels are shown for the lunasin-containing preparations obtained after ion-exchange chromatography and ultrafiltration (A) and after reverse phase chromatography (B). The red arrows indicate the protein band corresponding to lunasin.

degrees C until used. *Based on analysis of sodium dodecyl sulfate polyacrylamide gel electrophoresis (SDS PAGE) gels, this method yields lunasin at >98% purity.*

A key discovery made during the development of this method was that the majority of lunasin present in the crude extract is present in a protein complex that must be disrupted using a reducing agent such as DTT. Including the reducing step significantly increases the yield of lunasin. Preliminary pilot-scale purifications of lunasin using the new method have been completed with Kentucky BioProcessing (KBP, Owensboro, KY) to yield gram quantities of purified lunasin. *These results demonstrate that the method can be used for commercial scale production of lunasin. This represents a major breakthrough for the development of lunasin-based products.*

Transient Expression of Recombinant Lunasin

Previous studies demonstrated that lunasin cannot be expressed in prokaryotic or eukaryotic expression systems at levels required for product development or commercialization. This is likely due to the ability of lunasin to block mitosis. We have demonstrated that a tobacco mosaic virus (TMV)-based vector (GENEWARE®) can be used to express high levels of a GFP-lunasin fusion and for the first time, have established an expression system that has the potential to produce commercial-scale quantities of lunasin or modified forms of lunasin. This is a major development since this technology will provide a method for producing modified forms of lunasin that target specific cancer cells and/or have an increased ability to induce cancer cell death.

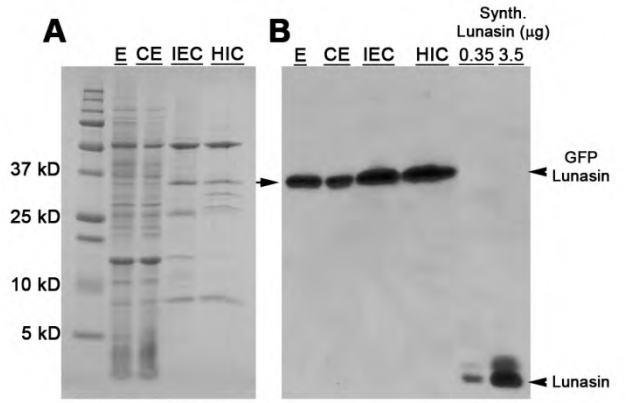

Figure 2. Expression of GFP-lunasin fusion in tobacco plants. Coomassie-stained SDS-PAGE gel (Panel A) and corresponding Western blot probed with a lunasin antibody (Panel B): crude extract (E), clarified extract (CE), ion-exchange chromatography purified fractions (IEC), and hydrophobic chromatography purified fractions (HIC). Synthetic lunasin was included as a control.

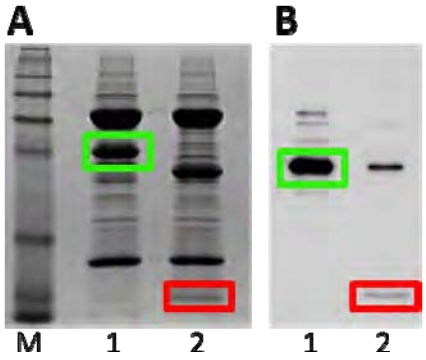

Figure 3. Release of lunasin from GFP-lunasin fusion by thrombin cleavage. Coomassie-stained SDS-PAGE gel (Panel A) and corresponding Western blot probed with a lunasin antibody (Panel B): Lane M, molecular weight standards; Lane 1, IEC-purified GFP-lunasin; Lane 2, IEC-purified GFP-lunasin treated with thrombin. The green boxes indicate the location of the GFP-lunasin fusion and the red boxes indicate the location of the released lunasin.

Our strategy is to generate a GFP-lunasin fusion protein that includes a linker between the GFP and lunasin components that contains a protease (thrombin) cleavage site. Thus, lunasin (or modified forms of lunasin) can be released by protease digestion and purified using our established methods for purifying native lunasin from white flake. Figure 2 demonstrates our ability to express and partially purify a GFP-lunasin fusion in tobacco plants. The expression levels are very good (~580 mg fusion per kg fresh weight plant tissue) and are suitable for commercial-scale production. Figure 3 demonstrates that cleavage of the fusion with thrombin releases lunasin. Approximately 90% of the fusion was cleaved and generated free GFP and lunasin. This result demonstrates that our strategy worked as planned and provides a method for producing modified forms of lunasin. *This technology will allow the production of more efficacious forms of lunasin as cancer therapeutics.* Our current efforts are aimed at completing the development of a method for purifying the GFP-lunasin fusion and to increase the efficiency of lunasin release by thrombin.

Development of Lunasin as a Chemoprevention Agent and Cancer Therapeutic

The primary objective of this aim was to confirm the anticancer activity of lunasin. Our preliminary experiments tested whether lunasin could prevent transformation of C3H/10T1/2 cells by treatment with a chemical carcinogen, 7,12-dimethylbenz[α]anthracene (DMBA). These studies verified the ability of lunasin to inhibit cellular transformation by DMBA. During the course of these studies, we also treated several established cancer cell lines with lunasin. Based on previous studies, we did not expect to see an effect. However, we observed that one cancer cell line exhibited significantly decreased growth after lunasin treatment, suggesting that the previously published conclusion that lunasin did not affect established cancer cell lines was incorrect. Based on this result, we focused our efforts on screening more cancer cell lines to see if we could identify additional cell lines that were sensitive to lunasin.

For these experiments, a panel of cancer cell lines was collected from colleagues or purchased from the American Type Culture Collection. Cells were grown in the appropriate medium and treated with 1-100 µM lunasin for 48 hours. Cell viability was assessed daily using a standard [3-(4,5-dimethylthiazol-2-yl)-5-(3-carboxymethoxy-phenyl)-2-(4-sulfo-phenyl)-2H-tetrazolium (MTS) assay (Promega). Table 1 summarizes the results to date. Of the seven lines tested, three exhibited significant sensitivity to lunasin treatment (H661, SW948, and WM115). The non-small cell lung cancer cell line H661 was the most sensitive, exhibiting a 77% reduction in viability after exposure to 100 µM lunasin for 48 hours. A graphical comparison of the effects of lunasin on the two most sensitive cell lines to an insensitive line is shown in Figure 4. These results clearly demonstrate that lunasin can induce cell death in specific cancer cell lines.

	Cell Viability (% Control)					
	24 hours			48 hours		
	1 µM	10 µM	100 µM	1 µM	10 µM	100 µM
H661	66.15	37.34	26.19	65.72	42.44	22.59
H1299	97.39	97.79	-	94.85	94.57	-
A549	100.23	102.48	102.14	100.66	93.76	85.80
SW948	97.95	86.96	67.63	72.49	67.63	62.33
SKBR3	95.67	99.28	99.23	99.92	97.88	101.72
A431	97.29	97.24	-	95.70	89.73	-
WM115	86.75	83.18	-	66.85	61.86	-

Table 1. Effect of lunasin on cancer cell viability. Cells were treated with the indicated concentrations of lunasin and cell viability determined using a MTS assay. Cell viability was calculated as follows: % Viability = Abs treatment/Abs untreated control ×100%. Cell lines tested: H661, non-small cell lung cancer; H1299, non-small cell lung cancer; A549, non-small cell lung cancer; SW948, adenocarcinoma, colorectal origin; SKBR3, adenocarcinoma, mammary gland origin; A431, epidermoid carcinoma; WM115, melanoma.

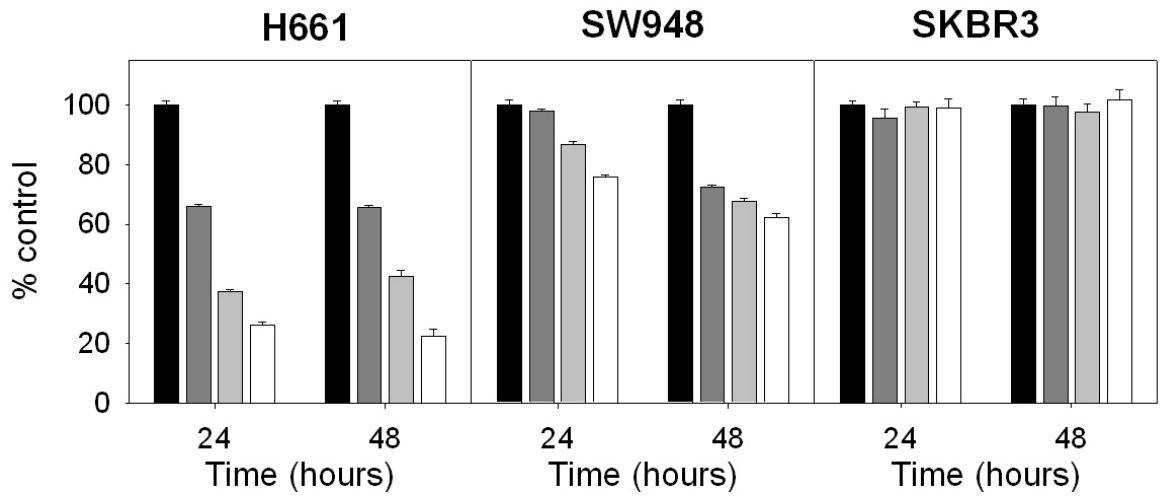

Figure 4. Effect of lunasin on cancer cell viability. Cells were cultured in the presence of 1 µM ( ), 10 µM ( ), or 100 µM ( ) lunasin for 24 and 48 hours, while control cells ( ) were treated with vehicle only. Cell viability was determined using the standard MTS assay. The data shown are the mean ± std. deviation of 3 replicate treatments. H661, non-small cell lung cancer; SW948, adeno-carcinoma, colorectal origin; SKBR3, adenocarcinoma, mammary gland origin.

Our results are consistent with recent studies that were published during the course of our studies that lunasin induces cell death in human breast cancer and leukemia cells.

Taken together, these studies demonstrate that there is the potential to develop lunasin into a cancer therapeutic for the treatment of specific cancer types. It remains an open question as to why only specific cancer cells are sensitive. Additional studies on the mode of action of lunasin are needed to address this important question.

Development of Antiviral Proteins as Microbicides (Dr. Kenneth Palmer)

This project represents an ongoing research program that Dr. Palmer established several years ago to develop uses for the algal-derived antiviral lectin, griffithsin (GRFT) as a preventive agent for HIV. GRFT is a lectin that binds specifically to clusters of high mannose glycans on the surface of many virus particles, frequently resulting in irreversible inactivation of the virus. We have developed a method to manufacture large quantities of the potent antiviral protein griffithsin (GRFT) in Nicotiana plants using a TMV-derived gene vector. Funds from the current award have been used to supplement other awards to pursue specific pilot projects related to expanding the use of GRFT as an antiviral agent.

Activity of GRFT against Viral Pathogens

Given that a number of important pathogenic viruses have envelopes containing high-mannose clusters, GRFT was tested against several other viral pathogens. We found that GRFT effectively inactivates SARS Coronavirus (SARS CoV) and protects animals against challenge with SARS-CoV as well as Ebola filovirus and highly pathogenic avian influenza. We evaluated antiviral activity of GRFT against a panel of emerging human and veterinary coronavirus pathogens, and established that GRFT has potent and broad-spectrum activity against all of the coronaviruses tested except mouse hepatitis virus. Consequently, we believe that GRFT is an interesting candidate drug for broad-spectrum antiviral prophylaxis against emerging viral pathogens as well as pathogens of strategic importance for biodefense. The results of these studies are presented in a recent publication (O'Keefe et al., 2010) provided in the Appendix. Future research will be focused on understanding the pharmacology and toxicology of GRFT formulated for administration via mucosal and parenteral routes, with the ultimate goal of evaluating its antiviral efficacy in animal models of coronavirus and filovirus infection.

Coupling of GRFT to a Solid Support

We have been evaluating the utility of antiviral lectin Griffithsin (GRFT) as a vaginal microbicide, and broad-spectrum antiviral. One key safety concern is whether GRFT binds non-specifically to host proteins, and if so what consequence the off-target binding has on the pharmacological and toxicological profile of GRFT-based drug candidates. We successfully coupled GRFT to Tosyl- and epoxy-activated magnetic beads and showed that GRFT coupled beads could extract HIV gp120, a model high mannose-bearing glycoprotein, from complex mixtures. These data show that GRFT may be coupled to a solid support without losing its lectin activity and that the magnetic beads have utility in both identifying "off-target" activity of GRFT. This discovery also

provides an opportunity to develop new products that potentially can be used for removing viruses from biological sources, such as blood.

Expression of the Antiviral Lectin MVL in *Nicotiana benthamiana*

A number of potentially antiviral lectins are produced by algae. We have begun to develop the potent antiviral lectin molecule (MVL) from blue-green alga *Microcystis viridis* to complement our studies using GRFT. It is possible that MVL will have a different activity spectrum than GRFT and that a combination of MVL and GRFT will be more potent than either lectin alone. Our studies to date have focused on determining whether MVL can be transiently expressed in tobacco. We have now cloned MVL into a recombinant TMV-based vector and have successfully expressed MVL in tobacco.

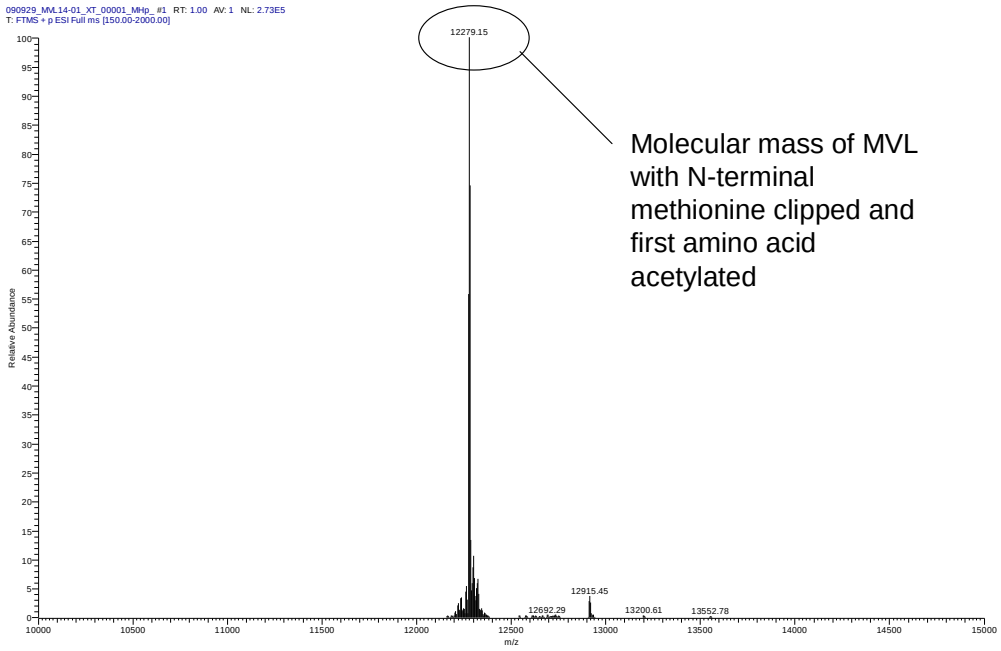

Figure 5: ESI-TOF Spectrum Confirms MVL Identity

Nicotiana benthamiana seedlings were inoculated with RNA transcripts of the rTMV::MVL construct. Within 7 days, *N. benthamiana* plants expressed very high levels of the MVL target protein. MVL could be extracted from *N. benthamiana* plants under acidic conditions (pH 4) and could be purified using a single chromatographic step using SP-sepharose. Product identity was verified using electrospray time of flight mass spectrometry methods (ESI-TOF; Figure 5). We have developed a microtiter plate-based HIV gp120 binding assay and showed that the MVL product could competes with other antiviral lectins, griffithsin (GRFT) and cyanovirin-N (CV-N) for similar binding sites. We are expanding this assay to determine MVL's binding affinity for influenza hemagglutinin. We obtained HIV inhibition data for MVL using an *in vitro* HIV pseudovirus infection system, which showed an IC50 (50% infection inhibition concentration) of approximately 33 nM.

Actinohivin and HIV (Dr. Nobuyuki Matoba)

The 12.5 KDa protein actinohivin is a type of lectin with a potent affinity to the glycan moiety of HIV gp120. This specific binding allows the protein to neutralize various primary HIV-1 isolates and HIV-2 viruses in the nanomolar range. A comprehensive binding study has shown that actinohivin, unlike many other anti-HIV lectins exemplified by cyanovirin-N, exclusively binds to a dense cluster of high-mannose glycans present on HIV and other viruses but not to other types of carbohydrate molecules. Because high-mannose clusters are not usually found in endogenous human proteins, actinohivin may have substantially fewer negative side effects upon topical application than other lectin microbicide candidates. The major goal of the current project is to utilize plant-based expression systems to produce actinohivin and to develop modified recombinant forms of actinohivin (rAH) that show improved capabilities of neutralizing HIV and potentially other enveloped viruses with high mannose glycans.

Summary of Major Accomplishments

Significant progress has been made in expressing rAH in tobacco plants. The major research milestones reached during the first year are summarized below. A paper has been submitted summarizing the achievements listed in 1 – 3, and 5 (see Appendix).

1. We demonstrated that functional rAH can be overexpressed in the cytosol of *Nicotiana benthamiana* plants within 4 – 5 days by the magnICON tobacco mosaic virus (TMV)-based expression system. The expression level reached up to 150 mg/kg of leaf materials, although this method caused substantial aggregation of rAH and a severe necrosis in leaves.

2. The rAH aggregation was significantly reduced by targeting the protein to the extracellular compartment (apoplast) through the endomembrane system.

3. The plant-expressed rAH showed anti-syncytia activity between HeLa cells expressing HIV-1 envelope and human CD4. This activity was comparable to that of native AH.

4. We tested a new AH construct, in which the small ubiquitin-like modifier (SUMO) protein was translatioanally fused to the N-terminus of AH. The SUMO protein has been shown to enhance and stabilize the expression of many otherwise “difficult to express” proteins in *E. coli* and other expression systems. We demonstrated that SUMO-AH can be expressed in the apoplast at up to ten times higher than AH, reaching ~200 mg/kg. Furthermore, this strategy has significantly lowered the necrotic reaction in leaves.

5. In collaboration with Dr. David Montefiori at Duke University Medical Center, we showed that AH-AH fusion, or a translational dimer of rAH (rdAH), possesses much

6. Using the above SUMO fusion strategy, rdAH was expressed in *N. benthamiana*. Similar to rAH, the dimer molecule was expressed at a high level in the apoplast.

Future worked will be focused on the following objectives:

Purification of plant-expressed rAH constructs. We will purify rAHs from *N. benthamiana* leaves and attempt to establish bulk production procedures that allow extensive preclinical evaluations of rAHs.

Engineering potent rdAH constructs. Given that the dimer of AH possesses significantly stronger anti-HIV-1 activity than the native monomer, we will create various rdAH constructs (e.g., modify the peptide linker connecting the two AH molecules) that exhibit better antiviral activity and plant expression capability.

Characterization of plant-expressed rAHs. Once purified, we will perform detailed biochemical, virological, and *in vitro* toxicological analyses of plant-expressed rAHs to examine their initial feasibilities toward candidate HIV-1 microbicides.

Regulation of Embryonic Stem Cell Pluripotency by the Mitochondrial Sulfhydryl Oxidase, Gfer (Dr. Uma Sankar)

Pluripotent embryonic (E) stem cells (SCs) are remarkable in their ability to undergo unlimited proliferation and self-renewal. Consequently, the capacity to proliferate indefinitely in culture in an undifferentiated state confer ESCs with considerable therapeutic potential, especially in the treatment of spinal cord injury and of degenerative diseases such as type 1 diabetes, Parkinson's and Alzheimer's. To preserve their pluripotency, ESCs in prolonged culture conditions must be protected from genomic, epigenetic, oxidative or mitochondrial damage. There are significant gaps in our knowledge regarding genes that execute the fundamental task of maintaining ESC stability and consequentially preserving their pluripotency in culture.

Growth factor *erv1*-like (Gfer) or augmenter of liver regeneration is the mammalian homologue of the evolutionarily conserved yeast erv1 protein, a flavin adenine dinucleotide (FAD)-dependent sulfhydryl oxidase predominantly located in the intermembrane space (IMS) of mitochondria. Although its precise function is unknown, Gfer plays roles in cytosolic Fe-S cluster assembly and mitochondrial biogenesis. In yeast, deletion of *erv1* is lethal with the mutants displaying aberrant mitochondrial morphology and defective biogenesis of Fe-S clusters. Moreover, Gfer is an important component of a disulfide redox relay system that mediates the import of proteins to the IMS of the mitochondria. Redox processes, such as the sulfhydryl oxidase activity of Gfer, are important regulators of intracellular enzyme activity, gene transcription and ultimately, of cell growth. Gfer was identified as one of 216 or 283 common genes that

are enriched in ESCs, neuronal (N) SCs and hematopoietic SCs. Gfer maps within the t-haplotype region of the SC gene-enriched mouse chromosome 17 and human chromosome 16, suggesting an evolutionary clustering of genes important in SC biology.

As no role has been established for Gfer in any stem cell, we used gene depletion and over-expression approaches to evaluate its role in the most primitive SCs, the pluripotent ESC. Down-regulation of Gfer in ESCs results in significantly reduced pluripotency marker gene expression, embryoid body formation, and growth. Depletion of Gfer also resulted in loss of ESC mitochondrial membrane potential ($_m$), fragmentation of mitochondria and autophagy of the damaged mitochondria (mitophagy). Conversely, mitochondria in ESCs over-expressing Gfer appeared significantly elongated, with well defined cristae. Interestingly, levels of the mitochondrial fission GTPase Drp1 were highly elevated in Gfer-KD cells and decreased in Gfer over-expressing cells, indicating that the enhanced Drp1 levels in Gfer-KD ESCs may be responsible for increased mitochondrial fragmentation, loss of $_m$ and apoptosis. Consistent with this idea, treatment with mdivi-1, a specific small molecule inhibitor of Drp1 or ectopic expression of a dominant negative K38A mutant of Drp1 ($Drp1^{DN}$) that inhibits GTP binding rescued mitochondrial dysfunction, apoptosis and pluripotency in Gfer-KD ESCs. A selective role for Gfer in SCs was corroborated by our observation that depletion of Gfer from differentiated cells such as primary mouse embryonic fibroblasts (MEFs) did not affect mitochondrial morphology, function or cell survival. Thus, during homeostasis, Gfer modulates the levels of Drp1 to preserve mouse ESC mitochondrial morphology and function; and maintain pluripotency marker expression in these primitive cells. These data provide novel information on the relationship of mitochondrial function to pluripotency or “stemness”; a very important, yet rather poorly understood aspect of stem cell (SC) biology.

Summary of Major Accomplishments

We completed our project investigating the role of Gfer in the regulation of ESC pluripotency. Our studies support an essential pro-survival role for Gfer in the maintenance of ESC pluripotency by preserving the structural and functional integrity of their mitochondria, through modulation of a key mitochondrial fission factor Drp1. Our studies are published in *Molecular Biology of the Cell Vol. 21, 1225–1236, April 1, 2010*.

During the upcoming year, we will strive to achieve the following goals: 1) elucidate the nature of regulation of Drp1 by Gfer and 2) investigate whether Gfer modulates mitochondrial dynamics and function in hematopoietic stem cells.

Programmatic and Infrastructure Accomplishments

Another emphasis of the current award was to make sure our research efforts were also supporting the development of the OCRP and the programmatic level. We established a series of goals to achieve over the three year funding period as outlined in the original Statement of Work. This goals and the progress to date are summarized below.

1) Complete the establishment of critical infrastructure needed to support OCRP research activities
   a) Purchase equipment required to conduct state-of-the-art molecular genetic and biochemical research

      This goal is on track and is being met. Specific equipment items required to support the research projects summarized in the previous sections, as well as new pilot projects, have been acquired and incorporated into the program.

   b) Provide major equipment needed to establish a rodent animal facility to support basic and preclinical research projects

      This goal has been removed due to the lack of funding to build a rodent facility at this time. The funds have been rebudgeted to other areas as described in the approved budget modification request.
   c) Provide core staff positions and research funds to provide basic laboratory research services and conduct pilot projects

      This goal is being met. Research scientists and student interns have been funded to conduct the research described. The scientific staff is now at a critical mass where continued progress is will be feasible as we move into year 2 of the award.
      .
2) Provide start-up funds for 2 new faculty to support the hiring of staff and the purchase of equipment, research supplies, and research services

   Start up funds have been provided for Dr. Matoba and have been adequate to meet his needs to establish a competitive research program. A second faculty hire is on hold while the University of Louisville identifies funds to support a new faculty position.

3) Support ongoing research projects being developed by OCRP faculty

   This goal is being met as evidenced by the significant progress that has been made by the OCRP faculty in moving research progress forward.

4) Collaborate with Kentucky BioProcessing (KBP), a local biotechnology company, on the development of PMPs, and promoting the development of the plant-based expression technologies
   a) Utilize KBP to provide process development and bioprocessing needs for OCRP projects

      This goal is being met. KBP has done several pilot-scale purifications of griffithsin and lunasin.

b) Develop collaborative projects with KBP and other PMP companies that offer opportunities to improve existing plant-based expression systems or to produce specific therapeutic proteins

Formal agreements for sharing research materials and knowledge have been established with KBP. Discussions are currently underway to establish specific joint research/training activities with KBP and a KBP client.

5) Establish collaborations with external research groups, including DOD and DOD-funded groups, aimed at utilizing plant-based expression systems to produce vaccines and therapeutics for infectious diseases and other biological warfare agents

Initial steps have been made to establish external collaborations. Dr. Palmer has put together a consortium of laboratories to facilitate the development of griffithsin for use against viral pathogens that are typically transmitted through inhalation.

The OCRP is very interested in developing collaborations with DOD scientists, however, to date, have found it difficult to identify appropriate partners. Renewed efforts will be initiated in year 2 to find specific research projects that OCRP faculty can contribute.

KEY RESEARCH ACCOMPLISHMENTS

Key accomplishments include:

- Significant advances in the development of lunasin as a cancer chemoprevention agent
    - Scalable purification method developed that will allow commercial-scale production of native lunasin from soybean
    - Development of a method to produce modified forms of recombinant lunasin using transient expression in tobacco
    - Demonstration that lunasin has the ability to inhibit the growth of specific cancer cells
- Continued development of griffithsin as an antiviral agent
    - Demonstration that griffithsin has activity against a range of enveloped viral pathogens including the SARS Coronavirus and ebola
    - Development of methods allowing griffithsin to be linked to solid supports that can be used to create filters and other solid materials for the removal of viruses from fluids
    - Establishment of a transient expression system for another antiviral lectin that will compliment the use of griffithsin
- Further advances in the development of the antiviral protein actinohivin

    - Improvements in the transient expression system to allow high level expression of stable protein
    - Demonstration that a dimerized form of actinohivin can be expressed and that it has higher antiviral activity than the monomer form
- Establishment of a project on embryonic stem cell pluripotency that will support the differentiation of neuronal stem cells
    - A key regulatory gene for stem cell function, Gfer, has been characterized
    - Determination that Gfer and calcium signaling is important for maintaining mitochondrial function

REPORTABLE OUTCOMES

The OCRP faculty has been very active in making presentations describing their work, submitting manuscripts for publication, submitting grant proposals, and protecting intellectual property developed during the course of developing specific research projects. These outcomes are summarized in the following sections:

Publications

Palmer KE, Jenson AB, Kouokam JC, Lasnik AB & Ghim SJ. Recombinant vaccines for the prevention of human papillomavirus infection and cervical cancer. *Experimental and Molecular Pathology* 86: 244-83, 2009. PMID: 19454268

Smith ML, Fitzmaurice WP, Turpen TH & Palmer KE. Display of peptides on the surface of Tobacco mosaic virus particles. *Current Topics in Microbiology and Immunology* 322: 31-41, 2009. PMID: 19401819

O'Keefe BR, Giomarelli B, Barnard DL, Shenoy SR, Chan PK, McMahon JB, Palmer KE, Barnett BW, Meyerholz DK, Wohlford-Lenane CL, McCray PB Jr.* Broad spectrum *in vitro* activity and *in vivo* efficacy of antiviral protein Griffithsin against emerging viruses of the family *Coronaviridae*. *Journal of Virology* 84(5):2511-21. PMID: 20032190

Pogue GP, Vojdani F, Palmer KE, Hiatt E, Hume S, Phelps J, Long L, Bohorova N, Kim D, Pauly M, Velasco J, Whaley K, Zeiltin L, Garger SJ, White E, Bai Y, Haydon H, Bratcher B. Production of pharmaceutical grade aprotinin and a recombinant monoclonal antibody product using plant-based transient expression systems. *Plant Biotechnology Journal* (accepted for publication, in press).

Matoba N, Davis KR, Palmer KE. Recombinant protein expression in *Nicotiana* plants. *Methods in Molecular Biology* (accepted for publication, in press).

Kouokam JC, Palmer KE. Plant-expressed griffithsin: a protein with potent, broad-spectrum effects against enveloped viruses. In *Medicinal Plant Biotechnology* (Arora R, editor). CAB International. (accepted for publication, in press).

Sharma S. M., Ostrowski M. C and Sankar U. Defective Co-activator Recruitment in Osteoclasts from *Microphthalmia-Oak Ridge* Mutant Mice. *Journal of Cellular Physiology* 220(1):230-7, 2009.

Todd L.R., Damin M. N., Gomathinayagam, R., Horn, S., Means A. R., and Sankar U. Growth factor erv1-like Modulates Drp1 to Preserve Mitochondrial Dynamics and Function in Mouse Embryonic Stem Cells. *Molecular Biology of the Cell Vol. 21, 1225–1236.*

Submitted

Monaco, S., Rusciano, M. R., McQuerry, K., Gomathinayagam, R., Todd, L. R., Sankar U. and Illario, M. Calmodulin dependent protein kinases II and IV antagonize each other in the regulation of leukemia cell proliferation. (In review)

Presentations

Invited Presentations and Research Seminars

Keith Davis

Development of Novel Vaccines and Therapeutics using Plant-Based Expression Systems. 2009. TATRC Product Line Review, Frederick, Maryland

Isolation and Analysis of the Cancer-Preventive Peptide Lunasin. 2009. Plant-Based Therapeutics Symposium, Sullivan University, Louisville, Kentucky

Kenneth Palmer

Invited by Virology Education NV to give oral presentation at 4th International HIV Transmission Workshop, Cape Town, South Africa. “Scaleable manufacture of HIV-1 entry inhibitor Griffithsin and validation of its safety and efficacy as a topical microbicide component.” July 17th, 2009.

Invited by United States Agency for International Development (USAID) and National Institute of Allergy and Infectious Diseases (NIAID) to give oral presentation on “Tobamovirus VLP Platform: Properties, Process Development and Manufacture Potential” at a Malaria Virus-Like Particles Development Workshop, Washington DC. September 22-23, 2009.

Invited seminar at Fraunhofer Center for Molecular Biotechnology, Newark DE. “Beyond Latex: Protecting Mucosal Surfaces Against Virus Infection” July 2009.

Invited seminar at University of Louisville Regional Biosafety Laboratory**.** “Griffithsin as a broad-spectrum antiviral”. August 2009

Nobuyuki Matoba

Invited Seminar, “BioProduction of Recombinant Protein Pharmaceuticals in Plants” Iwaki Meisei University, Fukushima, Japan, June 2009.

Invited Research Seminar, “Actinohivin, a Candidate HIV-1 Microbicide” Osaka University, Osaka, Japan, July 2009

Other Research Presentations/Posters

Keith Davis

Barnett, B.W., Seber, L.E., and Davis, K.R. 2009. Isolation and Analysis of the Cancer-Preventive Peptide Lunasin. Third International Conference on Plant-Based Vaccines & Antibodies: Plant Expression Systems for Recombinant Pharmacologics, Verona, Italy

Davis, K.R., Barnett, B.W., McConnell, E., and Seber, L.E. 2009. Development of the Soy-Derived Peptide Lunasin as a Chemopreventive Agent. Research! Louisville, University of Louisville, Louisville, Kentucky

Wermeling, R. and Davis, K.R. 2009. Seeking biomarkers for cadmium and NNK exposure in lung epithelial tissue. Research! Louisville, University of Louisville, Louisville, Kentucky

Seber, L.E., Barnett, B.W., Cai, J., and Davis, K.R. 2009.Development of the Peptide Lunasin as a Cancer Chemoprevention Agent. Eighth Annual Retreat, James Graham Brown Cancer Center, University of Louisville, Louisville, Kentucky (2nd Place, Roving Research Prize)

Kenneth Palmer

Lasnik AB, Smith ML, Willer S, Miller D, Ghim SJ, Jenson AB, Palmer KE. A plant produced L2 vaccines protects dogs against canine oral papillomavirus challenge. 25th International Papillomavirus Conferenc. Malmö, Sweden, May 2009

O’Keefe BR, Giomarelli B, Saucedo C, McRay P, Lear C, Olinger E, Palmer KE. Potent antiviral activity of the lectin Griffithsin. Fall American Chemical Society National Meeting and Exposition. Washington DC, August 2009

Palmer, KE, O’Keefe BR, Vojdani F, Buffa V, Shattock RJ, Montefiori DC, Hume SD, Bratcher B. Scaleable manufacture of HIV-1 entry inhibitor Griffithsin and validation of its safety and efficacy as a topical microbicide component. Plant-Based Therapeutics Symposium, Sullivan University. Louisville KY, July 2009.

Lasnik AB, Riedell SK, Smith ML, Waldron NW, Conway KV, Walker JM, Ditslear J, Franklin TE, Willer S, Ghim SJ, Jenson AB, Palmer KE. Plant-produced L2 vaccines induce protective immune responses against mucosotropic papillomavirus in the dog model, and HPV cross-neutralizing antibodies in immunized animals. Plant-Based Therapeutics Symposium, Sullivan University. Louisville KY, July 2009.

Palmer, KE, O'Keefe BR, Vojdani F, Buffa V, Shattock RJ, Montefiori DC, Hume SD, Bratcher B. Scaleable manufacture of HIV-1 entry inhibitor Griffithsin and validation of its safety and efficacy as a topical microbicide component. 4th International Workshop on HIV Transmission. Cape Town, South Africa, July 2009.

Koukam JC, Palmer KE Safety Evaluation of the potent anti-HIV lectin Griffithsin in cervico-vaginal cell models. Research!Louisville, Louisville KY. October 2009.

Walter W, Matoba N & Palmer KE Investigation of the binding specificity of antiviral lectin Griffithsin. Research!Louisville, Louisville KY. October 2009. (This poster won 3rd prize in the Medical Student Category)

Palmer KE Tobamovirus VLP Platform: Properties, Process Development and Manufacture Potential. Malaria Virus-Like Particles Development Workshop, Washington DC September 22-23, 2009

<u>Nobuyuki Matoba</u>

Barnett B, Conway H, Husk A, Pickel M, Arntzen C, Zhang P, Quinnan G, Mooney J, Hanson C, Takahashi A, Tanno K, Tanaka H, and Matoba N. Development of a robust and rapid plant expression system for Actinohivin, a novel anti-HIV-1 protein targeting the envelope high-mannose cluster. Plant-made Pharmaceuticals Meeting, Louisville/Owensboro, KY, June 2009

Matoba N, Barnett B, Husk A, and Conway H. Development of Plant-based HIV-1 Microbicides and Vaccines Targeting the Envelope High-mannose Clusters. Research!Louisville, University of Louisville, October 2009

Kessans SA, Frater J, Matoba N, and Mor TS. Plant expression of chimeric Gag/gp41 virus-like particles as a mucosally-targeted subunit vaccine against HIV-1. AIDS Vaccine 2009, Paris, France, October 2009 (Retrovirology 6: Supplement 3, P15)

Matoba N, Cherni I, Kessans S, Frater J, Preston K, Bomsel M, and Mor TS. Biochemical and immunological characterization of the plant-derived candidate HIV-1 mucosal vaccine CTB-MPR. AIDS Vaccine 2009, Paris, France, October 2009 (Retrovirology 6: Supplement 3, P182)

Matoba N, Barnett B, Husk A, Montefiori D, and Tanaka H. Development of Plant-based HIV Microbicides and Vaccines by targeting the High-mannose Cluster on the Env

Glycoprotein gp120. James Graham Brown Cancer Center 8th Annual Retreat, University of Louisville, November, 2009

Uma Sankar

Cary, R. and Sankar U. "Regulation of stem cell proliferation by a pro-quiescence kinase". 95th Annual Meeting of the Kentucky Academy of Sciences, November 13-14, Northern Kentucky University, Highland Heights, KY

McQuerry K. and Sankar U. "CaMKII Antagonizes CaMKIV to Enable Leukemia Cell Proliferation" Research! Louisville, October, 2009, Louisville, KY

Todd L. R., Damin M. N., Grant S. W., Means A. R and Sankar U. "Growth Factor *erv1* like (Gfer) Promotes Embryonic Stem Cell Function by Preserving Mitochondrial Integrity and Preventing Autophagic Cell Death. Keystone Symposium on Mitochondrial Dynamics and Physiology, March 22-27, 2009, Whistler, British Columbia, Canada.

Grant Applications

Agency/Number	Title	Role	PI	Project Period	Budget Request
Keith Davis					
NIH/3R01CA096997-04S1 (MPI)	A HER-2/neu pulsed DC1 vaccine for patients with DCIS	Co-PI	Brian Czerniecki U. Penn.	7/1/09 to 6/30/11	$2,963,392 Not Funded
Komen for the Cure	Development of Vaccines for Breast Cancer Prevention	Co-I	Brian Czerniecki U. Penn.	5/1/10 to 4/30/12	Subaward Budget $246,452 Not Funded
U of L Clinical and Translational Science Pilot Grant	Development of the Soy Peptide Lunasin as a Chemoprevention Agent	PI	Keith Davis	3/1/10 to 2/28/11	$89,122 Pending
Soybean Promotion Board	Development of the Soybean-Derived Peptide Lunasin as a Chemoprevention Agent	PI	Keith Davis	7/1/10 to 6/30/11	$68,020 Funded
Kenneth Palmer					
NIH/ R01 AI076169 Supplement	Antiviral Lectins as Microbicides	PI	Kenneth Palmer	09/15/09 to 08/31/10	$519,000 Funded
Gates Foundation Grand Challenges Explorations	Glycan targeting to protect against infectious disease	PI	Kenneth Palmer	05/01/10 to 04/30/11	$100,000 Not Funded
University of Louisville Clinical and Translational Research Pilot Grants	Selection of a pan-oncogenic HPV vaccine candidate	PI	Kenneth Palmer	03/01/10 to 02/28/11	$250,000 Pending

Agency/Number	Title	Role	PI	Project Period	Budget Request
Nobuyuki Matoba					
NIH NIAID R01	The Novel Mannose Cluster-Targeting Anti-HIV Protein Actinohivin	PI	Nobuyuki Matoba	01/01/10 to 12/31/14	$1,250,000 (direct costs) Not funded
NIH NIAID Microbicide Innovation Program V RFA (R21/R33 Phased Innovation Award)	Plant-produced Actinohivin as a Candidate HIV Microbicide	PI	Nobuyuki Matoba	04/01/10 to 03/31/15	$1,170,500 (direct costs) Priority Score: 37, Pending
Grand Challenges in Global Health/Grand Challenges Explorations Round 4	Development of a mucosal vaccine against enveloped viruses.	PI	Nobuyuki Matoba	05/01/10 to 04/31/11	$100,000 (direct costs) Not funded
UofL Clinical Translational Sciences Pilot Grant Program Basic Translational Research Award	A broad-spectrum vaccine against enveloped viruses.	PI	Nobuyuki Matoba	03/01/10 to 02/28/11	$49,020 (direct costs) Funded
Uma Sankar					
American Cancer Society Research Scholar Award	Role of calmodulin-dependent protein kinases in hematopoiesis and leukemia	PI	Uma Sankar	07/01/10 to 06/30/14	$964,969 (direct costs Scored Excellent Not funded
NIH NCI RO1	Calmodulin-dependent protein kinases in hematopoiesis and leukemia	PI	Uma Sankar	04/01/10 to 03/31/15	$1,250,000 (direct costs) Not funded

Invention Disclosures and Patent Applications

Purification of the Cancer Prevention Peptide Lunasin
Keith R. Davis, Brian Barnett, and Lauren Seber
Converted into USPO Provisional Patent Application (Serial No. 61/260,064)
LUNASIN-CONTAINING COMPLEX AND PURIFICATION OF LUNASIN FROM PLANTS
Inventors: Keith R. Davis, Brian Barnett, Lauren Seber, and Jian Cai

Expression of Lunasin in Plants
Keith R. Davis, Brian Barnett, and Lauren Seber
Converted into USPO Provisional Patent Application (Serial No. 61/254,788)
METHOD OF PRODUCING A LUNASIN POLYPEPTIDE IN PLANTS
Inventors: Keith R. Davis, Brian Barnett, and Lauren Seber

Compositions For Treating Papillomavirus Infection And Related Methods
Palmer, KE and Waldron NN.
Converted to USPO Provisional Patent Application (Serial No. 61/144,347)
COMPOSITIONS FOR TREATING PAPILLOMAVIRUS INFECTION AND RELATED METHODS
Inventors: Kenneth E. Palmer and N.N. Waldron

Highly mannosylated B subunit of cholera toxin as a potential broad-spectrum vaccine against enveloped viruses
Nobuyuki Matoba and Brian Barnett

CONCLUSION

During the first year of funding, the OCRP has made significant progress as a research organization and the faculty has utilized the support to make major progress in the implementation of specific research projects with relevance to DOD research priorities. Of note, the development of lunasin as a chemoprevention agent and/or therapeutic is now at the point where preclinical studies can be started as a prelude to potential clinical trials. The development of griffithsin has been significantly advanced, particularly with respect to indications other than HIV. It is anticipated that preclinical studies of griffithsin will be largely completed during the next two years using the additional support obtained from NIH. The projects on actinohivin and the regulation of stem cell development being developed by Drs. Matoba and Sankar, respectively, are progressing well. It is anticipated that the utility of actinohivin as an antiviral microbicide will be ascertained over the next year. Although the stem cell is the most basic project being supported, it has significant relevance to developing methods for controlling the differentiation of neuronal stem cells from embryonic stem cells. Specific product oriented research will be initiated when a clear target emerges from this preliminary work.

APPENDIX

Reprints and preprints of publications describing the work summarized in this report.

JOURNAL OF VIROLOGY, Mar. 2010, p. 2511–2521 Vol. 84, No. 5
0022-538X/10/$12.00 doi:10.1128/JVI.02322-09

Broad-Spectrum *In Vitro* Activity and *In Vivo* Efficacy of the Antiviral Protein Griffithsin against Emerging Viruses of the Family *Coronaviridae*▽

Barry R. O'Keefe,[1]* Barbara Giomarelli,[1] Dale L. Barnard,[2] Shilpa R. Shenoy,[3] Paul K. S. Chan,[4] James B. McMahon,[1] Kenneth E. Palmer,[5,6] Brian W. Barnett,[5] David K. Meyerholz,[7] Christine L. Wohlford-Lenane,[7] and Paul B. McCray, Jr.[8,9]*

Molecular Targets Development Program, Center for Cancer Research, NCI-Frederick, Frederick, Maryland 21702[1]; Utah State University, Logan, Utah[2]; SAIC-Frederick, Frederick, Maryland 21702[3]; Chinese University of Hong Kong, Hong Kong SAR, People's Republic of China[4]; James Graham Brown Cancer Center and Department of Pharmacology and Toxicology, University of Louisville, Louisville, Kentucky 40202[5]; Owensboro Cancer Research Program, Owensboro, Kentucky 42303[6]; and Departments of Pathology,[7] Pediatrics,[8] and Microbiology,[9] Carver College of Medicine, University of Iowa, Iowa City, Iowa 52242

Received 3 November 2009/Accepted 11 December 2009

Viruses of the family *Coronaviridae* have recently emerged through zoonotic transmission to become serious human pathogens. The pathogenic agent responsible for severe acute respiratory syndrome (SARS), the SARS coronavirus (SARS-CoV), is a member of this large family of positive-strand RNA viruses that cause a spectrum of disease in humans, other mammals, and birds. Since the publicized outbreaks of SARS in China and Canada in 2002-2003, significant efforts successfully identified the causative agent, host cell receptor(s), and many of the pathogenic mechanisms underlying SARS. With this greater understanding of SARS-CoV biology, many researchers have sought to identify agents for the treatment of SARS. Here we report the utility of the potent antiviral protein griffithsin (GRFT) in the prevention of SARS-CoV infection both *in vitro* and *in vivo*. We also show that GRFT specifically binds to the SARS-CoV spike glycoprotein and inhibits viral entry. In addition, we report the activity of GRFT against a variety of additional coronaviruses that infect humans, other mammals, and birds. Finally, we show that GRFT treatment has a positive effect on morbidity and mortality in a lethal infection model using a mouse-adapted SARS-CoV and also specifically inhibits deleterious aspects of the host immunological response to SARS infection in mammals.

The *Coronaviridae* are a group of enveloped positive-strand RNA viruses of the group *Nidovirales*. This group of viruses was not, until recently, of major concern as a matter of public health, although they were long recognized as important agents of serious disease in domestic and companion animals. The recent evidence of zoonotic transfer of this family of viruses from bats to animals such as palm civet cats and then to humans during the 2002-2003 outbreak greatly increased scientific interest in the *Coronaviridae* (7, 14, 19). The best-known coronavirus (CoV) is the causative agent of severe acute respiratory syndrome (SARS), termed the SARS-related coronavirus (SARS-CoV) (7, 14, 19). The lethal SARS outbreaks in China and Canada in 2002-2003 first brought SARS-CoV to public attention. The subsequent identification of two new human coronaviruses associated with acute respiratory infections in humans further illuminated the continuing potential threat that coronaviruses present to public health (31, 36).

Infection with SARS-CoV results from the binding of SARS-CoV spike glycoprotein (S) to angiotensin-converting enzyme 2 (ACE2) on the surface of susceptible cells in the lung followed by viral fusion with host cell membranes and transfer of virion contents into the cell (12, 25, 27). The infection stimulates significant cytokine responses in lung tissue that, together with pathologies associated with rapidly replicating virus, cause damage to the airway epithelium and alveolar membranes resulting in edema, respiratory distress, and (in ~10% of cases) death (5). Due to the proven threat from SARS-CoV infections and the possibility of future zoonotic transmission of coronaviruses, efforts have been initiated to identify agents that could either reduce infection or suppress the deleterious cytokine response to SARS-CoV infection (8, 29).

The molecular physiology of the SARS-CoV life cycle and the host response to infection have provided numerous potential targets for chemotherapeutic intervention. In addition to vaccine development strategies, various research groups have targeted the SARS-CoV-specific main protease or viral attachment, entry, and fusion for intervention. SARS-CoV protease inhibitors which inhibit the enzyme at concentrations from 0.5 to 7 μM have been reported (2). The SARS-CoV papain-like protease (PLP) has also been successfully developed as a target for small-molecule antivirals, some of which are active in the 100 nM range (22). Viral entry inhibitors include SARS-CoV S glycoprotein heptad repeat peptides identified as potential inhibitors of viral fusion (3). Another broad-spectrum antiviral

* Corresponding author. Mailing address for Barry R. O'Keefe: Bldg. 562, Rm. 201, NCI-Frederick, Frederick, MD 21702. Phone: (301) 846-5332. Fax: (301) 846-6872. E-mail: okeefeba@mail.nih.gov. Mailing address for Paul B. McCray, Jr.: 240 EMRB, Department of Pediatrics, University of Iowa, Iowa City, IA 52242. Phone: (319) 335-6844. Fax: (319) 335-6925. E-mail: paul-mccray@uiowa.edu.

▽ Published ahead of print on 23 December 2009.

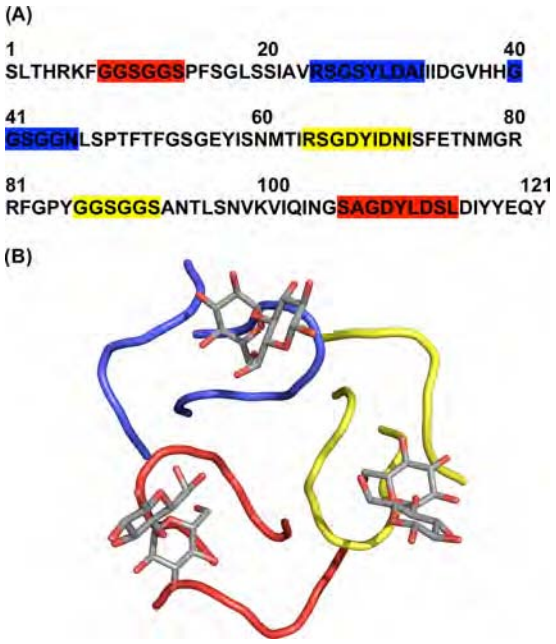

FIG. 1. The amino acid sequence and carbohydrate binding domains of griffithsin. Griffithsin monomers contain three distinct, nonlinear, and uniform binding sites for monosaccharides such as mannose and glucose. The binding sites (red, blue, and yellow) are shown both in the amino acid sequence of griffithsin (A) and binding to the disaccharide maltose in a three-dimensional representation derived from the X-ray crystal structure (B).

approach involves targeting the high-mannose oligosaccharides that are commonly found on viral surface glycoproteins. For example, carbohydrate-binding lectins, including *Urtica dioica* agglutinin (UDA), have been reported to bind to the SARS-CoV S protein and inhibit viral fusion and entry (33).

The antiviral protein griffithsin (GRFT) was originally isolated from the red alga *Griffithsia* sp. based upon its activity against the human immunodeficiency virus (HIV) (17). This unique 12.7-kDa protein was shown to bind specifically to oligosaccharides on the surface of the HIV envelope glycoprotein gp120. GRFT was shown to possess three largely identical carbohydrate-binding domains orientated as an equatorial triangle and affording multivalent binding and thereby increasing potency (37) (Fig. 1). Due to GRFT's ability to bind to specific oligosaccharides on envelope glycoproteins and block viral entry, it was hypothesized that GRFT might show broad-spectrum antiviral activity against other viruses, including SARS-CoV (38). Here we report the testing of GRFT for antiviral activity against a spectrum of coronaviruses, including SARS-CoV. In addition we present data on the specific binding interactions between GRFT and the SARS-CoV S protein. Finally, we evaluate the *in vivo* efficacy of intranasal administration of GRFT against infection with SARS-CoV in a lethal mouse model of pulmonary infection and explore the effects that GRFT treatment has on the induction of host cytokine response to SARS-CoV infection.

MATERIALS AND METHODS

***In vitro* antiviral testing methods. (i) Compounds.** Ribavirin was obtained from ICN Pharmaceuticals (Costa Mesa, CA). Multiferon (multisubtype, human alpha interferon [IFN-α], consisting of a1, a2, a8, a10, a14, and a21 human IFN-α subtypes) was kindly provided by Douglas Lind (Viragen Inc., Plantation, FL), and the SARS-CoV protease inhibitor was provided by Sui Xiong Cai (Maxim Pharmaceuticals, San Diego, CA). GRFT was produced by recombinant production in *Nicotiana benthamiana* and purified for use as reported previously (18). SARS-CoV spike glycoprotein was obtained through the NIH Biodefense and Emerging Infections Research Resources Repository, NIAID, NIH (SARS-CoV spike [S] protein with histidine tag, recombinant from baculovirus, NR-686). ACE2 was purchased from R & D Systems (Minneapolis, MN). Recombinant HIV-1_{IIIB} gp120, produced in a baculovirus expression system, was purchased from Immunodiagnostics Inc. (Woburn, MA).

(ii) Cells and virus. Human ileocecal colorectal human adenocarcinoma cells (HRT-18G), mouse embryonic liver cells (BNL), and human diploid fibroblast cells (MRC-5) obtained from the American Type Culture Collection (ATCC, Manassas, VA) were grown in Dulbecco's modified essential medium (DMEM) supplemented with 10% fetal bovine serum (FBS; HyClone Laboratories, Thermo-Fisher Scientific, Logan, UT) and 0.37% $NaHCO_3$. Chicken embryonic fibroblast cells (UMNSAH/DF-1, East Lansing line), pig testis fibroblast cells (ST), human ileocecal colorectal human adenocarcinoma cells (HCT-8), and African green monkey kidney cells (Vero 76), all from the ATCC, were grown in Eagle's formulation of minimal essential medium (MEM) supplemented with 10% FBS and 0.22% $NaHCO_3$ and propagated at 37°C.

Calf diarrheal virus (bovine coronavirus [BCoV]) was obtained from the ATCC and passaged in HRT-18G cells. Infectious bronchitis virus strain Connecticut A5968 (IBV; ATCC) was routinely grown in DF-1 cells. Mouse hepatitis virus (MHV) strain JHM (ATCC) and porcine transmissible gastroenteritis virus strain Miller (PCoV; ATCC) were passaged in BNL cells and ST cells, respectively. Human coronavirus strain OC43 (HCoV-OC43; ATCC) was passaged in HCT-8 cells (ATCC), and human coronavirus strain 229E (HCoV-229E; ATCC) was passaged in MRC-5 cells. The following reagent was obtained through the NIH Biodefense and Emerging Infections Research Resources Repository, NIAID, NIH: human coronavirus, NL63 (Amsterdam 1), NR-470. NL63 was grown in rhesus monkey kidney cells (LLC-MK2 cells) in MEM supplemented with 5% FBS, later reduced to 2% FBS in antiviral assays Severe acute respiratory syndrome-associated coronavirus strain Urbani (SARS-CoV) was obtained from the Centers for Disease Control and Prevention (Atlanta, GA), the Tor-II strain was from Heinz Feldman (National Microbiology Laboratory, Winnipeg, Manitoba, Canada), the Frankfurt strain was from Jindrich Cinatl (Klinikum der J. W. Goethe Universität, Frankfurt am Mein, Germany), and the CuHK strain was from Paul K. S. Chan (Chinese University of Hong Kong, Hong Kong, People's Republic of China). They were all passaged in Vero 76 cells. When viruses were grown, the FBS in each medium used above was reduced to 2% and the $NaHCO_3$ was reduced to 0.22% with the exception of BCoV. For BCoV, the growth and antiviral test media were MEM without serum, 0.18% $NaHCO_3$, 20 IU trypsin/ml, 2.0 μg EDTA/ml. For all antiviral assays, 50 μg/ml gentamicin was also added to the antiviral test medium.

(iii) Preparation of compounds for testing. Compounds in solution were diluted in test medium (MEM without serum) through a series of eight 1/2-$\log_{10}$ dilutions for evaluation. A positive-control drug was also included to ensure that an overwhelming amount of virus was not used in the assay. The latter compounds also were diluted in test medium as described above.

(iv) CPE inhibition assay. Cells were seeded into 96-well flat-bottomed tissue culture plates (Corning Glass Works, Corning, NY), 0.2 ml/well, at the proper cell concentration, and incubated overnight at 37°C in order to establish a cell monolayer. When the monolayer was established, the growth medium was decanted and the various dilutions of test compound were added to each well (3 wells/dilution, 0.1 ml/well). Compound diluent medium was added to cell and virus control wells (0.1 ml/well). Virus (viral multiplicity of infection [MOI] = 0.01 to 0.001), diluted in test medium, was added to compound test wells (3 wells/dilution of compound) and to virus control wells at 0.1 ml/well. Virus was added approximately 5 min after compound. Test medium without virus was added to all toxicity control wells (2 wells/dilution of each test compound) and to cell control wells at 0.1 ml/well. The plates were incubated at 37°C or at 33°C (HCoV-OC43, HCoV-299E, and HCoV-NL63) in a humidified incubator with a 5% CO_2-95% air atmosphere until virus control wells had adequate cytopathic effect (CPE) readings. This was achieved in 3 to 10 days after virus exposure to cells, depending on the virus. Cells were then examined microscopically for CPE, this being scored from 0 (normal cells) to 4 (maximal, 100% CPE). The cells in the toxicity control wells were observed microscopically for morphological changes attributed to cytotoxicity. This cytotoxicity was also graded as T (100% toxicity, complete cell sloughing from plate), P_{VH} (80% cytotoxicity), P_H (60% cytotoxicity), P (40% cytotoxicity), P_{SI} (20% cytotoxicity), and 0 (normal cells). The 50% effective dose (EC_{50}) and 50% cytotoxic dose (IC_{50}) was calculated by

regression analysis of the virus CPE data and the toxicity control data, respectively. The therapeutic index (SI) for each compound tested was calculated using the formula $SI = IC_{50}/EC_{50}$.

(v) NR uptake assay of CPE inhibition and compound cytotoxicity. The neutral red (NR) uptake assay was done on the same CPE inhibition test plates as described above to verify the inhibitory activity and the cytotoxicity observed by visual observation. The NR assay was performed using a modified method of Cavanaugh et al. (4) as described by Barnard et al. (1). Medium was removed from each well of a plate, 0.034% NRF (0.34% neutral red in phosphate-buffered saline [PBS] supplemented with formalin at 10%) was added to each well of the plate, and the plate was incubated for 2 h at 37°C in the dark. The NR solution was then removed from the wells and rinsed, and the remaining dye was extracted using ethanol buffered with Sörenson's citrate buffer. Absorbances at 540 nm/405 nm were read with a microplate reader (Opsys MR; Dynex Technologies, Chantilly, VA). Absorbance values were expressed as percentages of untreated controls and EC_{50}, IC_{50}, and SI values were calculated as described above.

(vi) ELISA studies. The binding of GRFT to SARS-CoV spike (S) glycoprotein was analyzed in enzyme-linked immunosorbent assay (ELISAs) with two different modalities. For standard ELISA, purified S protein was immobilized at 10 ng/well to a 96-well protein-binding plate (Nunc; Maxisorp) by incubation for 2 h at room temperature. After being rinsed twice with PBS containing 0.1% Tween (PBS-T) and three times with blocking buffer (Superblock buffer in PBS containing 0.05% Tween 20; Pierce, Rockford, IL), the plate was incubated with blocking buffer for 3 h at room temperature and rinsed again with PBS-T. The wells were then incubated with 0.5 $\log_{10}$ serial dilutions of GRFT, followed by anti-GRFT rabbit polyclonal antibodies for 1 h at room temperature. After washing with PBS-T, the amount of bound GRFT was determined by adding a 1:5,000 dilution of goat anti-rabbit–horseradish peroxidase (HRP; Immuno-Pure). The plate was washed again, and horseradish peroxidase substrate (Kirkegaard & Perry Laboratories) was added. The reaction was stopped by the addition of 50 μl/well of 2 M H_2SO_4, and absorbance was measured at 450 nm. To measure the inhibition of binding of GRFT to S protein by mannose, increasing concentrations of mannose were added to 100-μl aliquots of GRFT (1 μM in PBS) or PBS alone and incubated at room temperature for 30 min on a rocker. The aliquots were then added to an S-protein-coated plate and incubated for 1 h at room temperature. Binding of GRFT was measured as described above.

In studies to measure the ability of GRFT to prevent the binding of S protein to the ACE2 cellular receptor, S protein was bound to the wells of a 96-well plate as above and then, after blocking and washing, was treated with increasing concentrations of GRFT (0.0003 to 100 pmol/well). Following incubation with GRFT (2 h), the plate was then incubated with 50 ng/well of recombinant ACE2 (R & D Systems) and incubated for 1 h prior to washing and visualization with primary polyclonal goat-anti-ACE2 antibodies followed by horseradish peroxidase-ligated mouse anti-goat secondary antibodies monitored by absorbance at 450 nm.

(vii) Isothermal titration calorimetry. The calorimetric binding experiments were carried out on a VP-ITC microcalorimeter (MicroCal, Inc., Northampton, MA). In the experiments, 5-μl aliquots of a GRFT solution (289.3 μM) were injected from a 250-μl syringe into a rapidly mixing (300 rpm) solution of either SARS-CoV spike (1.8 μM) or HIV-1_{IIIB} gp120 (2.5 μM) contained within the calorimetric cell (1.4426 ml). Both experiments were carried out at 25°C in 10 mM sodium phosphate buffer, 60 mM NaCl, 0.02% NaN_3 (pH 7.0). The isotherms were corrected for dilution/buffer effects and fitted using the Origin ITC analysis software according to the manufacturer's protocols. Concentrations of all proteins were determined by amino acid analysis. A nonlinear least-square method was used to fit the titration data and to calculate the errors. From the binding curve, values for enthalpy, stoichiometry, and binding affinity were extracted. The other thermodynamic parameters (free energy of binding and entropy values) were calculated using $\Delta G = -\mathrm{RTlnKa}$, $\Delta G = \Delta H - T\Delta S$, and $R = 1.985$ cal/(mol · K), where R is the universal gas constant, T is temperature in Kelvin, and K_a is the reaction equilibrium constant.

***In vivo* mouse testing methods. (i) Animals.** Six- to eight-week-old BALB/c female mice were purchased from NCI. The animals were maintained in an approved animal care facility and transferred to a biosafety level 3 (BSL3) facility prior to infection. This study was approved by the University of Iowa Animal Care and Use Committee. The animals used for this study were part of a four-armed experiment including sham-treated, positive-control (SARS-CoV-infected), griffithsin-treated, and rhesus theta-defensin-treated animals. The results with rhesus theta-defensin-treated and some of the positive-control and sham-treated animals were previously published (34).

(ii) Griffithsin administration. Recombinant GRFT protein was prepared as described previously (18). Mice were lightly anesthetized, and GRFT (5 mg/kg of body weight/day) was delivered intranasally 4 h prior to administration of MA15 SARS-CoV, followed by 2 doses daily (2.5 mg/kg/dose) for 4 days following infection. This dose was adopted from a previous study of a similar viral entry inhibitor, cyanovirin-N, with influenza virus (28).

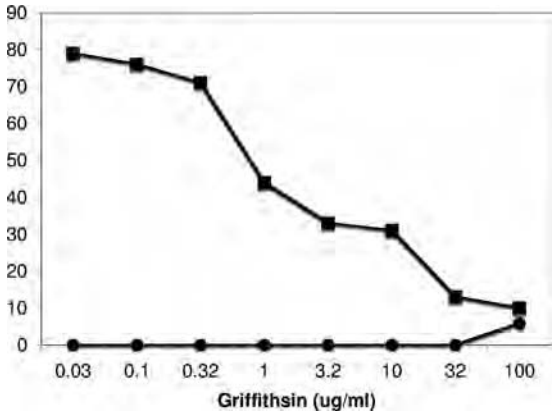

FIG. 2. The effect of griffithsin against SARS-CoV (Urbani strain) in cell culture. Griffithsin inhibited the cytopathic effects of SARS-CoV on Vero cells in a concentration-dependent manner (■) while displaying minimal toxicity to the same cells in the absence of viral challenge (●).

(iii) MA15 Urbani SARS-CoV infection. Mice were anesthetized and inoculated intranasally with 3×10^5 PFU of mouse-adapted Urbani SARS-CoV (MA15) (23) in 30 μl sterile 1× PBS in an approved BSL3 facility. Mice were weighed and examined daily. Animals were euthanized if they lost >25% of their body weight. To obtain specimens for lung histology, virus titers, lung homogenates, and serum collection, mice were euthanized at baseline and at day 2, day 4, and day 10 postinfection (p.i.). The left lung was fixed in zinc formalin, and the right lung was homogenized and stored at −80°C.

(iv) Plaque assay. The right lung was excised aseptically, placed in sterile 1× PBS, and homogenized manually with a tissue homogenizer. The homogenates were centrifuged at 12,000 rpm for 10 min, and supernatant was removed. Lung homogenate supernatants were diluted and applied to Vero cells and incubated for 1 h, and an overlay medium containing agarose was added to cell surface. Three days postinfection, cells were fixed in 10% formaldehyde and stained with 0.1% crystal violet. Formed plaques were counted.

(v) Immunohistochemistry. To detect SARS-CoV antigen, zinc formalin-fixed paraffin sections were incubated with a monoclonal antibody to the SARS-CoV N protein (gift of John Nicholls, University of Hong Kong, Hong Kong) and expression was detected using a biotin-avidin system. Sections were examined and photographed under light microscopy.

(vi) Histopathology. Fixed tissues were processed, paraffin embedded, sectioned (4 μm), and hematoxylin and eosin stained. All slides were screened by a veterinary pathologist to first identify the histopathologic parameters that were appreciably altered. Subsequently, the slides were scored in a blinded fashion for lesion severity. Edema scores included the following: 1, absent to rare; 2, mild, detectable foci of eosinophilic seroproteinaceous fluid within alveoli and airways; and 3, moderate to severe foci of eosinophilic seroproteinaceous fluid pooling in alveoli and airways. Perivascular cellular inflammation scores included the following: 1, absent to rare; 2, mild perivascular cellular infiltrates starting to form small cellular aggregates; and 3, moderate to severe perivascular cellular infiltrates often forming marked aggregates with variable disruption of adjacent tissue architecture. Necrotizing bronchiolitis scores included the following: 1, absent to rare; 2, scattered foci of airway epithelium necrosis and sloughing; and 3, multifocal and coalescing to circumferential airway epithelium necrosis and sloughing. Data from the mice used in the negative-control (sham-treated) and positive-control (SARS-CoV without GRFT) groups were included in a previously published study (35).

(vii) Multiplex cytokine assay. To identify changes in cytokine protein expression, we performed a multiplex bead-based immunoassay using the Bio-Plex cytokine assay (Bio-Rad Laboratories) as previously reported (35). Lung tissue homogenates were studied at baseline and day 2, day 4, and day 10 postinfection. The Bio-Plex cytokine 23-Plex kit measured mouse interleukin-1α (IL-1α), IL-1β, IL-2, IL-3, IL-4, IL-5, IL-6, IL-9, IL-10, IL-1(p40), IL-12(p70), IL-13, IL-17, eotaxin, granulocyte colony-stimulating factor (G-CSF), granulocyte/macrophage CSF (GM-CSF), IFN-α, KC, monocyte chemoattractant protein 1 (MCP-

TABLE 1. Antiviral activity of griffithsin against distinct strains of SARS-CoV

Strain	EC_{50} (μg/ml)	IC_{50} (μg/ml)	SI
Urbani	0.61	>100	>164
Tor-II	0.61	>100	>164
CuHK	0.78	>100	>128
Frank	1.19	>100	>83

1), MIP-1α, MIP-1β, RANTES, and tumor necrosis factor alpha (TNF-α) expression patterns and was used following the manufacturer's instructions. Fifty microliters of each lung tissue homogenate specimen was transferred to appropriate microtiter wells containing diluted antibody-coated bead complexes and incubation buffer. Samples were incubated for 30 min at room temperature and 18 h (both in the dark) at 4°C, with continuous shaking. Following a rinse with wash buffer, 25 μl detection antibody was added to each well, incubated for 30 min at room temperature (in the dark), and washed as described above. Next 50 μl of streptavidin-phycoerythrin was added to all wells and incubated for 10 min at room temperature (in the dark). All microtiter wells received a final wash, and beads were resuspended in 125 μl assay buffer and analyzed on the Bio-Plex suspension array system using Bio-Plex Manager software. Cytokine concentrations were automatically calculated based on standard curve data. Data from the mice used in the negative-control (sham-treated) and positive-control (SARS-CoV without GRFT) groups were included in a previously published study (35).

(viii) Statistical analysis. The indicated statistical tests were used in experimental analyses. Student's *t* test was applied at the 95% confidence level ($P < 0.05$) to each paired comparison at each of their respective time points using Excel. Analysis of variance (ANOVA) was applied with Bonferroni correction for multiple comparisons.

RESULTS

GRFT inhibits *in vitro* infection of *Coronaviridae*. In initial studies of the effect of GRFT against SARS-CoV (Urbani strain), GRFT was shown to potently inhibit the cytopathic effect of SARS-CoV on Vero 76 cells (38). As can be seen in Fig. 2, GRFT reduced the percentage of cells killed by SARS-CoV (Urbani) in a concentration-dependent manner (EC_{50} = 48 nM) while showing minimal toxicity to the control cells. The antiviral activity of GRFT against SARS-CoV was not limited to the Urbani strain of the virus, as three additional strains of SARS-CoV were also sensitive to GRFT at similarly low concentrations (Table 1). In addition, GRFT demonstrated activity against a broad spectrum of other coronaviruses that infect mammals and birds in testing using a variety of cell lines. Of the coronaviruses tested several were susceptible to inhibition by GRFT below the lowest dose utilized (~1 nM) (Table 2). It is interesting that GRFT mutants, in which the carbohydrate-binding domains were altered to prevent carbohydrate binding, were largely inactive against coronaviruses (EC_{50} of >50 μg/ml) (data not shown). Though all of the human coronaviruses were sensitive to GRFT at nanomolar concentrations, two coronaviruses, infectious bronchitis virus (IBV) and HCoV (NL63), were the most sensitive to inhibition (EC_{50} of <2.5 nM and <0.25 nM, respectively). It is interesting that these viruses belong to the group 1 and group 3 phylogenetic groups of the *Coronaviridae*, respectively. NL63 uses the ACE2 recep-

TABLE 2. Activity of GRFT on the cytopathic effects of selected coronaviruses[a]

Virus, host, and treatment compound	Cytopathic effect assay			Neutral red uptake assay		
	EC_{50}	IC_{50}	SI	EC_{50}	IC_{50}	SI
BCoV in human ileocecal colorectal human adenocarcinoma cells (HRT-18G)						
GRFT	0.057	32	560	<0.032	>100	>3,100
Ribavirin	0.32	50	313	<0.32	30	94
IBV (Connecticut A5968) in chicken embryonic fibroblast cells (UMNSAH/DF-1)						
GRFT	<0.032	68	>2,100	<0.032	>100	>3,100
Multiferon	0.0,012	>0.03	>25	0.0,029	>0.03	>10
MHV (JHM) in mouse embryonic liver cells (BNL)						
GRFT	0.23	0.44	1.9	0.13	2.5	19
Multiferon	0.001	>0.3	>290	0.0,012	>0.3	>260
PCoV (Miller) in pig testis fibroblast cells (ST)						
GRFT	0.57	57	100	0.77	46	59
Multiferon	0.000,095	>0.03	>320	0.00,017	>0.03	>180
HCoV (OC43) in human ileocecal colorectal human adenocarcinoma cells (HCT-8)						
GRFT	0.16	52	320	0.048	>100	>2,100
Multiferon	0.0,006	>0.03	>50	0.0,008	>0.03	>37
HCoV (229E) in human diploid fibroblast cells (MRC-5)						
GRFT	0.18	>10	>56	0.33	>10	>30
Ribavirin	18	>1,000	>56	26	>1,000	>38
HCoV (NL63) in rhesus monkey kidney cells (LLC-MK2)						
GRFT	<0.0,032	10	>3,100	<0.0,032	>10	>3,100
Ribavirin	0.63	320	500	1.6	120	77

[a] EC_{50}s and IC_{50}s are shown in micrograms per milliliter for GRFT and ribavirin and in international units per milliliter for multiferon.

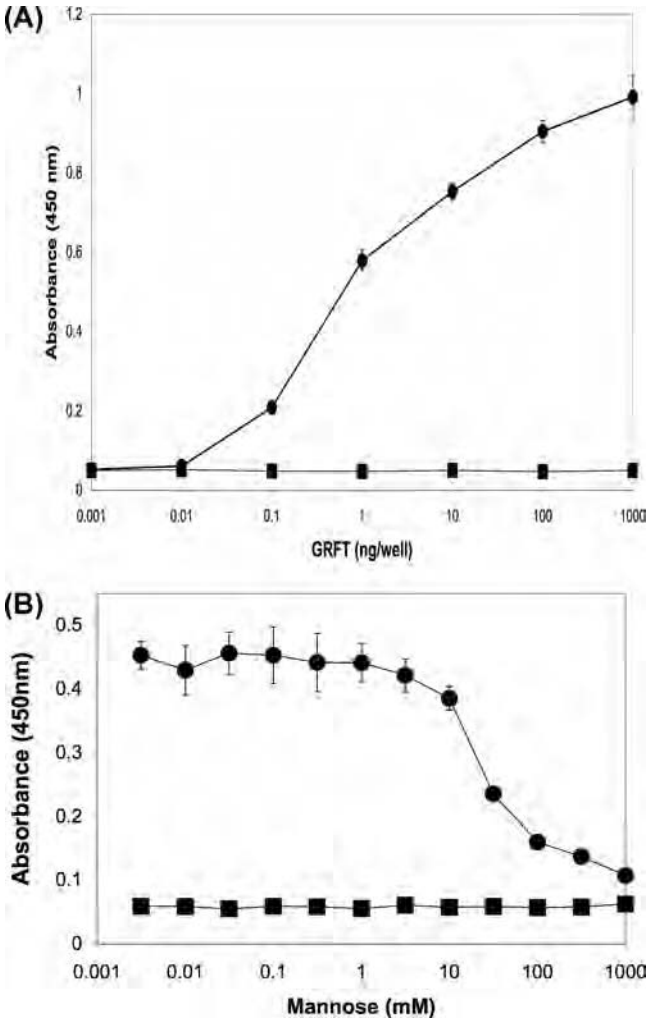

FIG. 3. Griffithsin binds directly to SARS-CoV spike glycoprotein in a carbohydrate-dependent manner. Griffithsin bound directly to recombinant SARS-CoV spike protein (produced in a baculovirus expression system) (●) (A), and this binding was shown to be inhibited by increasing concentrations of mannose (●) (B) compared to the bovine serum albumin controls (■) (A and B).

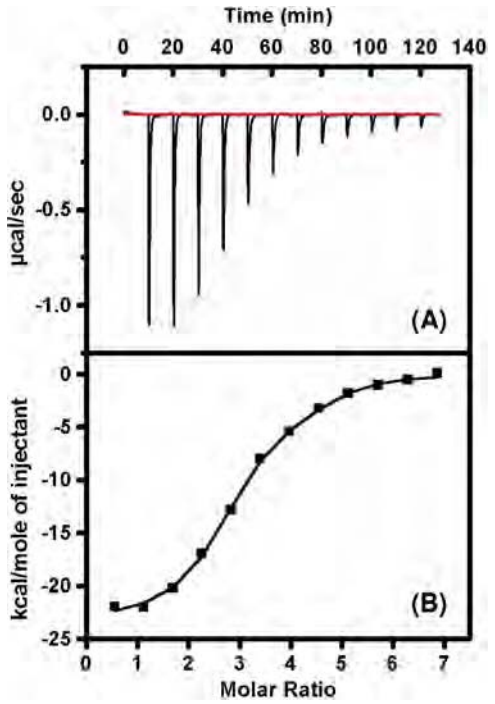

FIG. 4. Isothermal titration calorimetry measuring the binding interaction between GRFT and SARS-CoV spike glycoprotein. (A) Heat of interaction of multiple injections of GRFT into a solution of SARS-CoV spike shows a saturable binding interaction between GRFT and S. (B) Plotted thermogram of the saturable binding of GRFT and SARS-CoV spike from which affinity constants and stoichiometry are determined. The other thermodynamic parameters (free energy of binding and entropy values) were calculated using $\Delta G = -\mathrm{RTlnKa}$, $\Delta G = \Delta H - T\Delta S$, and $R = 1.985$ cal/(mol · K). (Table 3 has more data.)

tor for binding (21), but IBV uses a receptor possessing α-2,3-linked sialic acid residues (34). Thus, at the receptor level, the two viruses appear to have nothing in common, other than their susceptibility to inhibition by carbohydrate-binding agents such as GRFT (13, 32). In addition, GRFT was shown to be active against both group 1 and 2 *Coronaviridae* which utilize different mechanisms for proteolytic cleavage of the spike glycoprotein (9).

GRFT binds directly to the SARS-CoV spike glycoprotein. To determine if the activity of GRFT against SARS-CoV was due to specific interactions with the spike glycoprotein, ELISA studies utilizing recombinant SARS-CoV spike glycoprotein were performed which showed that GRFT binds to this protein in a concentration-dependent manner (Fig. 3A). Additional experiments showed that this binding interaction could be inhibited by the addition of excess mannose, thereby indicating that the association between GRFT and SARS-CoV spike glycoprotein is carbohydrate dependent (Fig. 3B). It should be noted, however, that the expression of the SARS-CoV spike glycoprotein in a baculovirus expression system could alter its glycosylation. Finally, ELISA studies were performed to determine if the binding of GRFT to SARS-CoV S glycoprotein was sufficient to inhibit the subsequent binding of the host cell receptor human ACE2 to S. These studies indicated that GRFT was unable to significantly inhibit the binding of the SARS-CoV S glycoprotein to ACE2 (data not shown). The inability of GRFT to inhibit S binding to ACE2 is similar to previous results with HIV-1 in which GRFT did not significantly inhibit the binding of gp120 to CD4 (17).

GRFT binds to SARS-CoV spike glycoprotein at multiple sites with high affinity. Since previous studies with carbohydrate-binding proteins and HIV gp120 have shown the importance of multiple binding interactions between these proteins and specific oligosaccharides on the envelope glycoprotein (26), we undertook isothermal titration calorimetric studies with recombinant SARS-CoV spike and GRFT. The results of this experiment provided the binding stoichiometry between these two proteins and also showed that GRFT interactions with spike are enthalpically driven (Fig. 4), resulting in a dissociation constant (K_d) of 24.9 nM (Table 3). The binding interaction of GRFT with SARS-CoV S was compared to that of GRFT with HIV-1 gp120. The results show that GRFT has an ~10:1 binding stoichiometry with gp120 compared to a 3:1

TABLE 3. Thermodynamic parameters of GRFT-spike and GRFT-gp120 binding interactions

Envelope protein	Affinity, K_d (nM)	Enthalpy, ΔH (kcal/mol)	Entropy ($T\Delta S$) (kcal/mol)	Free energy (ΔG^a) (kcal/mol)	Stoichiometry (GRFT:Env protein)
HIV-1 gp120	8.2 ± 4.3	−30.40 ± 0.26	−19.16 ± 0.28	−11.20 ± 0.28	10.46 ± 0.18
SARS CoV spike	24.9 ± 2.0	−23.10 ± 0.50	−12.76 ± 0.50	−10.40 ± 0.05	2.97 ± 0.12

[a] $\Delta G = -RTlnKa$.

binding stoichiometry with S, a finding which suggests a greater presence of high-mannose oligosaccharides on gp120 than on S. In line with the greater binding enthalpy (ΔH) for GRFT with gp120, the dissociation constant for gp120 was tighter (8.2 nM) than that seen with S.

GRFT pretreatment prevents lethal pulmonary infection in mice. The mouse-adapted MA15 SARS-CoV causes a dose-dependent lung disease and significant morbidity and mortality in BALB/c mice (23). Groups of mice were inoculated with 3×10^5 PFU of virus, a dose previously shown to cause at least 75% mortality (35). One group of mice received concomitant treatment with intranasally administered GRFT peptide as described in Materials and Methods. As shown in Fig. 5A, MA15-infected mice began to lose weight within 2 to 3 days of inoculation, and this continued until they died from the infection or recovered. Figure 5B shows the survival curve for sham-treated, SARS-CoV-infected, and GRFT-treated mice. In contrast to the outcomes in untreated mice, animals that received GRFT 4 h before inoculation with MA15 followed by twice-daily treatment for 4 days did not lose weight and exhibited 100% survival. Animals receiving sham treatment or GRFT treatment alone survived and exhibited no weight loss. We evaluated MA15 titers in lung tissue 0, 2, and 4 days postinoculation. As shown in Fig. 5C, GRFT treatment significantly diminished the tissue virus titers on day 2 postinfection (mean virus titers [PFU/g tissue]: GRFT plus SARS-CoV, day 2, 4.2×10^6, and day 4, 2.9×10^6; SARS-CoV alone, day 2, 8.5×10^7, and day 4, 1.1×10^7). In agreement with this observation, GRFT-treated animals also had reduced pulmonary viral antigen load assessed by localization of the SARS-CoV N gene antigen by immunohistochemistry (Fig. 6).

GRFT treatment decreases pulmonary pathology during SARS-CoV infection. In humans and animal models SARS-CoV causes significant pathological changes in pulmonary tissues, characterized by necrotizing bronchiolitis, perivascular cellular inflammation, and alveolar edema (7, 14, 23). We assessed pulmonary histopathology at 2, 4, and 10 days postinfection in untreated, sham-treated (no virus), and GRFT-treated animals. Mice receiving GRFT alone developed a modest level of perivascular infiltrate that was largely resolved

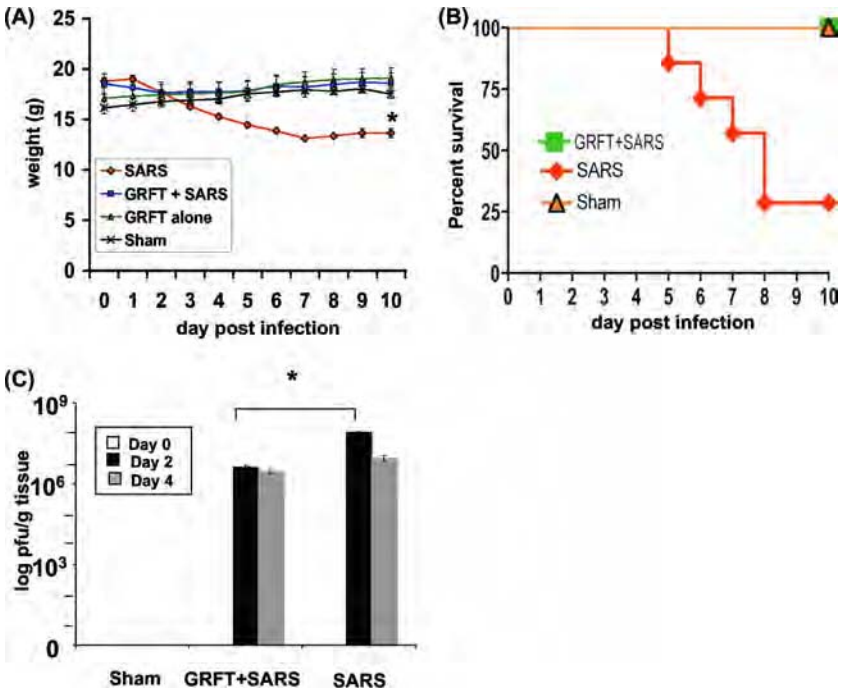

FIG. 5. GRFT treatment protects mice against morbidity from SARS-CoV infection. Mice were treated with sham control (no virus), GRFT alone, SARS-CoV alone, or GRFT followed with SARS-CoV infection as described in Materials and Methods. Animals were monitored daily for weight loss (A) and survival (B). GRFT-treated mice exhibited no weight loss. SARS-CoV-infected mice without GRFT treatment had a 30% survival rate and a ~25% decrease in weight in those that survived. Lung tissue was harvested from mice, and viral titer levels were determined (C). Results in panels A and C are presented as means ± standard errors. $n = 7$ in panels A and B, and $n = 3$ in panel C. *, $P \leq 0.05$ by t test or ANOVA.

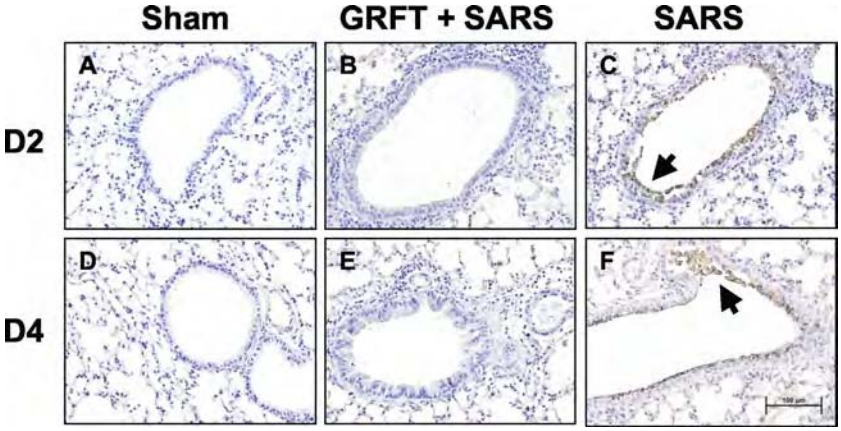

FIG. 6. SARS N gene product in lung tissue. Antigen labeling (brown stain) was detected primarily in lungs infected with SARS-CoV at day 2 and day 4 postinfection (C and F), mainly in airway epithelial cells and sloughed cells within the airway lumen (indicated by arrows) compared to lungs treated with vehicle (A and D). Lungs treated with GRFT and infected with SARS-CoV exhibited limited N antigen expression (B and E). $n = 3$ at each time point. Scale bar = 100 μM.

by 10 days (6 days following the last dose of GRFT) (Fig. 7). In contrast, mice treated with SARS-CoV alone manifested necrotizing bronchiolitis, perivascular infiltrates, and alveolar edema that were resolving by 10 days postinfection (in surviving animals). While mice receiving GRFT treatment and SARS-CoV exhibited robust perivascular infiltrates at levels greater than those with SARS-CoV alone, possibly due to the increased immunogenicity of GRFT-aggregated viral particles, the GRFT-treated mice had reduced levels of pulmonary edema at both 2 and 4 days postinfection and reduced severity of necrotizing bronchiolitis at 2 days postinfection. The histopathology scores are presented graphically in Fig. 8.

GRFT treatment modifies cytokine responses in infected lung tissue. It has been hypothesized that the morbidity and mortality associated with SARS-CoV infection originate from maladaptive cytokine/chemokine responses or suppression of innate immune responses (6, 20). We measured cytokine levels in pulmonary tissue homogenates 2 and 4 days following MA15 inoculation. As shown in Fig. 9 (top panels), mice treated with GRFT and exposed to SARS-CoV showed significantly reduced levels of MIP-1α at day 2 postinfection compared to SARS-CoV alone. IL-1α and -β, RANTES, MCP-1, IL-12(p40), IL-6, and G-CSF also showed downward trends in GRFT-treated mice compared to SARS-CoV at day 2 p.i., but the differences were not statistically significant. At 4 days p.i. (Fig. 9, bottom panels), several cytokines were significantly reduced in GRFT-treated animals compared to those infected with SARS-CoV alone, including IL-1α and -β, IL-6, G-CSF, MCP-1, and IL-12(p40).

DISCUSSION

The potent antiviral lectin GRFT displayed low nanomolar activity against SARS-CoV (Urbani strain) with an EC_{50} of 0.61 μg/ml (48 nM). Previously, we had speculated that GRFT would be likely to have activity against SARS-CoV due to its

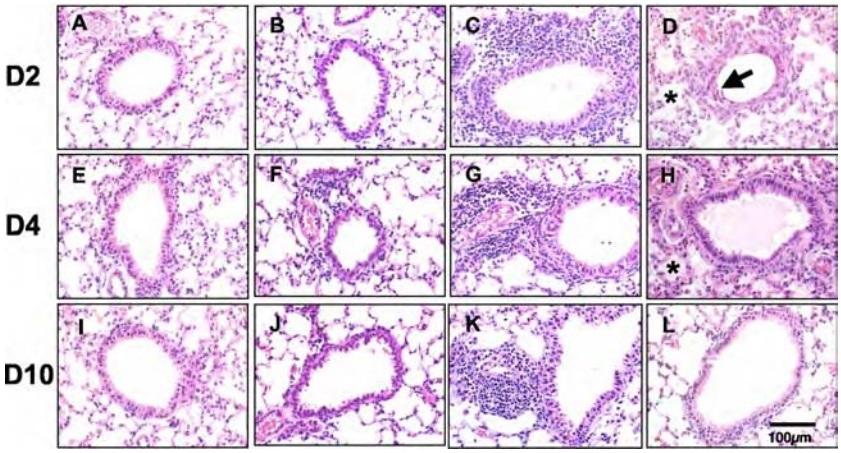

FIG. 7. Lung tissue histopathology in SARS-CoV-infected mice with or without GRFT treatment. Hematoxylin-and-eosin-stained tissues were examined 2, 4, and 10 days postinfection. See Results for additional experimental details. Representative histopathology in sham-treated (A, E, and I), GRFT control-treated (B, F, and J), and SARS-CoV-infected mice with (C, G, and K) or without (D, H, and L) GRFT treatment. Arrows indicate necrotizing bronchiolitis; asterisks indicate alveolar edema. $n = 4$ at each time point. Scale bar = 100 μM.

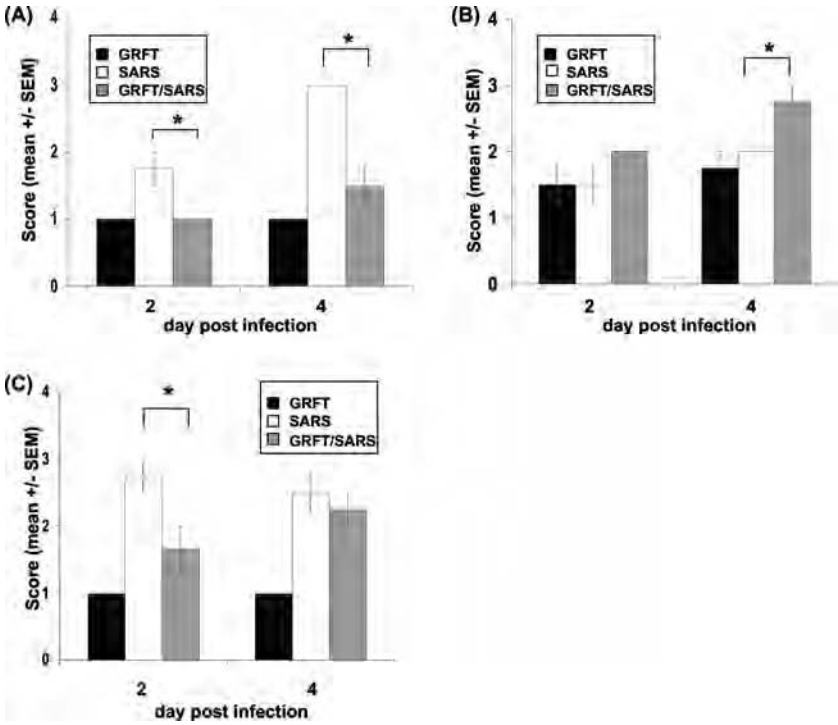

FIG. 8. Pulmonary histopathology scores in SARS-CoV-infected mice with or without GRFT treatment. Tissues were harvested 2 and 4 days postinfection and scored as described in Materials and Methods for evidence of alveolar edema (A), perivascular cellular infiltrates (B), and necrotizing bronchiolitis (C). Results are presented as means ± standard errors. $n = 4$; *, $P \leq 0.05$, by two-way ANOVA with Bonferroni posttest correction.

carbohydrate specificity and the known carbohydrate components of the SARS-CoV envelope glycoprotein S (17). Extending our previous work (38), here we detail the activity of GRFT against several strains of SARS-CoV and show consistent advantageous selectivity indices for all of the tested strains (Table 1). The carbohydrate-binding agent *Urtica dioica* agglutinin (UDA) has been reported by others to display anti-SARS-CoV activity (33), but the concentrations necessary for inhibition were significantly higher than those that we report here for GRFT. This difference in activity could be attributed to the multivalent interactions that the three independent carbohydrate-binding sites afford GRFT (Fig. 1). Other agents reported to show activity against SARS-CoV, including SARS-CoV protease inhibitors (2) and SARS-specific heptad repeat peptides (3), also show such activity only at significantly higher molar concentrations than GRFT. Though human recombinant alpha interferon (multiferon) and other host-targeted agents have demonstrated anti-SARS activity at low concentrations (Table 2), their potency does not significantly exceed that displayed by GRFT, which directly targets viral envelope glycoproteins.

In addition to GRFT's activity against SARS-CoV, GRFT demonstrated broad-spectrum activity against a variety of *Coronaviridae*, including those recently identified as human pathogens (Table 2). Both group 1 and group 2 coronaviruses were susceptible to GRFT with similarly low nanomolar sensitivities. GRFT was active against coronavirus strains that utilize protein-protein interactions for viral targeting (e.g., ACE2 as a cellular receptor, SARS-CoV, and HCoV-NL63) and those that utilize protein-carbohydrate interactions for viral attachment (i.e., α-2,3-linked sialic acid moieties, IBV-CoV, and HCoV-OC43). The broad range of *Coronaviridae* species sensitive to GRFT is a significant attribute for this antiviral protein, as this group of viruses appears to be capable of continuing zoonotic evolution and transfer to human hosts (24). GRFT was active against several coronaviruses at concentrations less than the lowest tested concentration, with HCoV-NL63, a strain recently identified as a human pathogen (31), displaying the greatest sensitivity (EC_{50} of <0.0032 μg/ml [0.25 nM]).

The molecular target through which GRFT appears to mediate its anticoronavirus activity is the surface envelope glycoprotein spike (S). GRFT binds directly to S as shown by ELISA studies showing the concentration-dependent binding to recombinant S (Fig. 3A). This mechanism is consistent with our previous studies of the mechanism of GRFT inhibition of HIV that revealed that GRFT binds to HIV-1 gp120 and prevents viral entry (18, 38). As with gp120, GRFT appears to bind to S *via* interaction with oligosaccharide moieties. Here we show that the binding of GRFT to S can indeed be inhibited by millimolar concentrations of mannose (Fig. 3B). GRFT is known to bind to select monosaccharides (mannose, glucose, and *N*-acetylglucosamine) in a multivalent manner *via* its three independent carbohydrate-binding domains (Fig. 1) (37). The unique equatorial triangular orientation of these three sites has been shown to be ideally situated so as to allow for engagement of multiple triantennary arms of specific high-mannose oligosaccharides such as oligomannose 9 (38). The oligo-

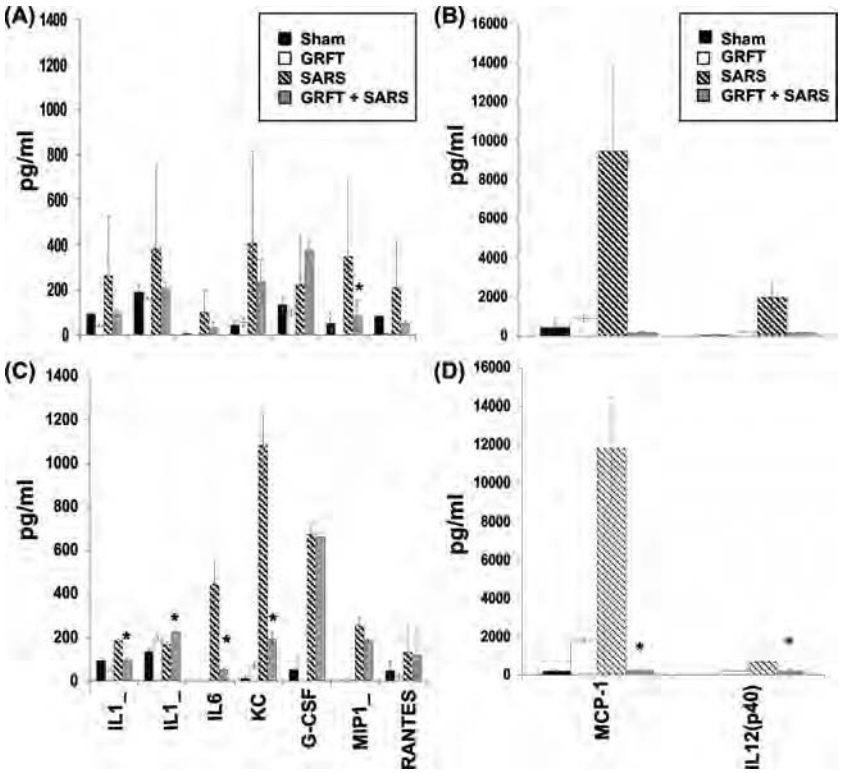

FIG. 9. GRFT modifies pulmonary cytokine responses to SARS-CoV infection. Tissues were harvested at days 2 (A and B) and 4 (C and D) postinfection, and cytokine responses were assessed by multiplex analysis of tissue homogenates as described in Materials and Methods. Results are shown for sham (PBS alone), GRFT alone, SARS-CoV with GRFT treatment, and SARS-CoV alone. The *x* axis legend for day 4 applies to the corresponding panels above for day 2. Note differences in scale on left and right panels. Results are presented as means ± standard errors. $n = 3$/group; *, $P \leq 0.05$ by *t* test.

saccharide component of SARS-CoV S has been previously reported to contain multiple high-mannose oligosaccharides to which GRFT might bind (11). In isothermal titration calorimetry studies of the GRFT/S binding interactions, we determined that GRFT binds to S with a stoichiometry of 3:1, indicating that there are multiple binding sites for GRFT on S (Table 3). In this same study GRFT was shown to bind to S with a dissociation constant of 24.9 nM (Table 3). This affinity is weaker than that between GRFT and HIV gp120, an interaction that was shown to have a stoichiometry of ~10:1. The difference in the affinity for GRFT between the two envelope glycoproteins is likely responsible for the difference seen in the antiviral activity of GRFT against HIV (0.048 to 0.63 nM) (17) and SARS-CoV (48 to 94 nM). Finally, we found that GRFT does not inhibit the interaction between the SARS-CoV S protein and the cellular receptor ACE2 (data not shown). Thus, the interaction between GRFT and S results in a complex that, though still able to bind to ACE2, may prevent the subsequent steps necessary for viral entry. The activity of GRFT against IBV suggests that this perturbation of viral entry by GRFT may be independent of the specific cellular receptor to which S binds. This mechanism would be similar to that seen with GRFT and HIV wherein GRFT binding to gp120 does not prevent the subsequent binding of gp120 to the cellular receptor CD4 and where GRFT activity is independent of the chemokine receptor tropism (CCR5 or CXCR4) of individual strains of HIV-1 (17, 34).

The potent *in vitro* activity of GRFT against SARS-CoV was confirmed using a mouse model system recently shown to recapitulate several aspects of the physiology of human disease, including a robust pulmonary disease component (23, 24). This mouse model was previously used to examine the impact of prior infection with SARS-CoV on immune responses and survival following subsequent reexposure to the virus (23, 24). Previously our group has shown that intranasal administration of the antiviral lectin cyanovirin-N (CV-N) was efficacious in the prevention of mortality in mice infected with a lethal strain of influenza virus H1N1 (28), and so, for the current study, GRFT was administered to mice *via* an intranasal route.

These studies showed that GRFT protected mice from a lethal inoculum of mouse-adapted SARS-CoV. Remarkably, 100% of the animals treated with 10 mg/kg/day GRFT survived viral challenge, in contrast to only 30% of control animals (Fig. 5B). The improved survival was further mirrored by prevention of weight loss and an improvement in lung histopathology scores and a reduction in lung tissue virus titers (Fig. 5A and C and Fig. 8), which indicated that, though GRFT-treated animals were infected by SARS-CoV, drug treatment significantly modified the disease course and outcome.

While studies of the prevention or treatment of SARS-CoV lung disease have been hampered by the lack of animal models that faithfully recapitulate the features of human disease, several agents have shown some efficacy in modifying disease outcomes. These include alpha interferon (10), small interfer-

ing RNA (siRNA) (15), and passive immunization (16, 30). Furthermore, in a previous study we showed that, during a simultaneous experiment, the cyclic antimicrobial peptide rhesus theta-defensin did not afford the complete protection from the morbidity of SARS-CoV infections seen with GRFT (34). Our studies with a robust model of SARS-CoV lung disease suggest that GRFT may modify disease outcome by more than one mechanism. First, by binding to the spike glycoprotein and interfering with productive infection, GRFT may reduce the overall virus burden during the first and subsequent rounds of infection. The reduced virus load in the lung at days 2 and 4 is consistent with this idea. In addition, enhanced peribronchial mononuclear cell infiltration and modification of cytokine responses suggest that GRFT also is immunomodulatory. Stimulation of leukocyte infiltration has been reported following high-dose topical application of GRFT to rabbit (but not human) cervical mucosa (18).

GRFT is currently being developed for potential use as an anti-HIV microbicide, and a recent report demonstrates the feasibility of large-scale production and purification from *Nicotiana benthamia* plants (18). This new production stream for GRFT greatly enables future development efforts based on GRFT's activity against enveloped viruses. Here we report that GRFT shows remarkable efficacy against lethal SARS-CoV infection and was potently active against a broad spectrum of human coronaviruses and other animal coronaviruses. Several questions remain, however, for the potential development of GRFT for use in the treatment of respiratory infections by coronaviruses. Though GRFT completely protected animals from SARS-CoV-induced death, the presence of perivascular infiltrates in GRFT-treated animals will need to be further characterized. Since GRFT-treated infected animals recover, this suggests that these cellular infiltrates may mediate protective immunity to SARS-CoV. Further, we used 10-mg/kg/day GRFT treatment in the *in vivo* studies reported here, but it is possible that lower doses of GRFT treatment would be equally efficacious. In summary, the antiviral protein GRFT shows noteworthy activity against *Coronaviridae* mediated *via* a novel mechanism of action. Its outstanding *in vivo* efficacy in SARS-CoV-infected mice suggests that this antiviral agent merits further investigation for the prophylaxis or treatment of respiratory infection by susceptible viruses.

ACKNOWLEDGMENTS

We thank T. Moulaei and A. Wlodawer (Macromolecular Crystallography Laboratory, CCR, NCI) for assistance with the figures. We thank K. Gustafson and J. Beutler (MTDP, CCR, NCI), T. Gallagher (Loyola University), and S. Perlman (University of Iowa) for their reviews and helpful discussions of the manuscript.

This research was supported by the Intramural Research Program of the NIH, National Cancer Institute, Center for Cancer Research (B.R.O., B.G., and J.B.M.). This project has been funded in whole or in part with federal funds from the National Cancer Institute, National Institutes of Health, under contract N01-CO-12400 and HHSN261200800001E (S.R.S.). P.B.M. is supported in part by NIH PO1 A1060699 and the Roy J. Carver Trust; K.E.P. is supported by a Pilot Project grant from the Executive Vice President of the University of Louisville.

The content of this publication does not necessarily reflect the views or policies of the Department of Health and Human Services, nor does mention of trade names, commercial products, or organizations imply endorsement by the U.S. Government.

REFERENCES

1. **Barnard, D. L., C. W. Day, K. Bailey, M. Heiner, R. Montgomery, L. Lauridsen, P. K. Chan, and R. W. Sidwell.** 2006. Evaluation of immunomodulators, interferons and known in vitro SARS-coV inhibitors for inhibition of SARS-coV replication in BALB/c mice. Antivir. Chem. Chemother. **17:**275–284.
2. **Blanchard, J. E., N. H. Elowe, C. Huitema, P. D. Fortin, J. D. Cechetto, L. D. Eltis, and E. D. Brown.** 2004. High-throughput screening identifies inhibitors of the SARS coronavirus main proteinase. Chem. Biol. **11:**1445–1453.
3. **Bosch, B. J., B. E. Martina, R. Van Der Zee, J. Lepault, B. J. Haijema, C. Versluis, A. J. Heck, R. De Groot, A. D. Osterhaus, and P. J. Rottier.** 2004. Severe acute respiratory syndrome coronavirus (SARS-CoV) infection inhibition using spike protein heptad repeat-derived peptides. Proc. Natl. Acad. Sci. U. S. A. **101:**8455–8460.
4. **Cavanaugh, P. F., Jr., P. S. Moskwa, W. H. Donish, P. J. Pera, D. Richardson, and A. P. Andrese.** 1990. A semi-automated neutral red based chemosensitivity assay for drug screening. Invest. New Drugs **8:**347–354.
5. **Chen, J., and K. Subbarao.** 2007. The immunobiology of SARS*. Annu. Rev. Immunol. **25:**443–472.
6. **de Lang, A., T. Baas, T. Teal, L. M. Leijten, B. Rain, A. D. Osterhaus, B. L. Haagmans, and M. G. Katze.** 2007. Functional genomics highlights differential induction of antiviral pathways in the lungs of SARS-CoV-infected macaques. PLoS Pathog. **3:**e112.
7. **Drosten, C., S. Gunther, W. Preiser, S. van der Werf, H. R. Brodt, S. Becker, H. Rabenau, M. Panning, L. Kolesnikova, R. A. Fouchier, A. Berger, A. M. Burguiere, J. Cinatl, M. Eickmann, N. Escriou, K. Grywna, S. Kramme, J. C. Manuguerra, S. Muller, V. Rickerts, M. Sturmer, S. Vieth, H. D. Klenk, A. D. Osterhaus, H. Schmitz, and H. W. Doerr.** 2003. Identification of a novel coronavirus in patients with severe acute respiratory syndrome. N. Engl. J. Med. **348:**1967–1976.
8. **Golda, A., and K. Pyrc.** 2008. Recent antiviral strategies against human coronavirus-related respiratory illnesses. Curr. Opin. Pulm. Med. **14:**248–253.
9. **Gorbalenya, A. E., L. Enjuanes, J. Ziebuhr, and E. J. Snijder.** 2006. Nidovirales: evolving the largest RNA virus genome. Virus Res. **117:**17–37.
10. **Haagmans, B. L., T. Kuiken, B. E. Martina, R. A. Fouchier, G. F. Rimmelzwaan, G. van Amerongen, D. van Riel, T. de Jong, S. Itamura, K. H. Chan, M. Tashiro, and A. D. Osterhaus.** 2004. Pegylated interferon-alpha protects type 1 pneumocytes against SARS coronavirus infection in macaques. Nat. Med. **10:**290–293.
11. **Han, D. P., M. Lohani, and M. W. Cho.** 2007. Specific asparagine-linked glycosylation sites are critical for DC-SIGN- and L-SIGN-mediated severe acute respiratory syndrome coronavirus entry. J. Virol. **81:**12029–12039.
12. **Jia, H. P., D. C. Look, L. Shi, M. Hickey, L. Pewe, J. Netland, M. Farzan, C. Wohlford-Lenane, S. Perlman, and P. B. McCray, Jr.** 2005. ACE2 receptor expression and severe acute respiratory syndrome coronavirus infection depend on differentiation of human airway epithelia. J. Virol. **79:**14614–14621.
13. **Keyaerts, E., L. Vijgen, C. Pannecouque, E. Van Damme, W. Peumans, H. Egberink, J. Balzarini, and M. Van Ranst.** 2007. Plant lectins are potent inhibitors of coronaviruses by interfering with two targets in the viral replication cycle. Antiviral Res. **75:**179–187.
14. **Ksiazek, T. G., D. Erdman, C. S. Goldsmith, S. R. Zaki, T. Peret, S. Emery, S. Tong, C. Urbani, J. A. Comer, W. Lim, P. E. Rollin, S. F. Dowell, A. E. Ling, C. D. Humphrey, W. J. Shieh, J. Guarner, C. D. Paddock, P. Rota, B. Fields, J. DeRisi, J. Y. Yang, N. Cox, J. M. Hughes, J. W. LeDuc, W. J. Bellini, and L. J. Anderson.** 2003. A novel coronavirus associated with severe acute respiratory syndrome. N. Engl. J. Med. **348:**1953–1966.
15. **Li, B. J., Q. Tang, D. Cheng, C. Qin, F. Y. Xie, Q. Wei, J. Xu, Y. Liu, B. J. Zheng, M. C. Woodle, N. Zhong, and P. Y. Lu.** 2005. Using siRNA in prophylactic and therapeutic regimens against SARS coronavirus in Rhesus macaque. Nat. Med. **11:**944–951.
16. **McCray, P. B., Jr., L. Pewe, C. Wohlford-Lenane, M. Hickey, L. Manzel, L. Shi, J. Netland, H. P. Jia, C. Halabi, C. D. Sigmund, D. K. Meyerholz, P. Kirby, D. C. Look, and S. Perlman.** 2007. Lethal infection of K18-hACE2 mice infected with severe acute respiratory syndrome coronavirus. J. Virol. **81:**813–821.
17. **Mori, T., B. R. O'Keefe, R. C. Sowder II, S. Bringans, R. Gardella, S. Berg, P. Cochran, J. A. Turpin, R. W. Buckheit, Jr., J. B. McMahon, and M. R. Boyd.** 2005. Isolation and characterization of griffithsin, a novel HIV-inactivating protein, from the red alga Griffithsia sp. J. Biol. Chem. **280:**9345–9353.
18. **O'Keefe, B. R., F. Vojdani, V. Buffa, R. J. Shattock, D. C. Montefiori, J. Bakke, J. Mirsalis, A. L. d'Andrea, S. D. Hum., B. Bratcher, C. J. Saucedo, J. B. McMahon, G. P. Pogue, and K. E. Palmer.** 2009. Scaleable manufacture of HIV-1 entry inhibitor griffithsin and validation of its safety and efficacy as a topical microbicide component. Proc. Natl. Acad. Sci. U. S. A. **106:**6099–6104.
19. **Peiris, J. S., S. T. Lai, L. L. Poon, Y. Guan, L. Y. Yam, W. Lim, J. Nicholls, W. K. Yee, W. W. Yan, M. T. Cheung, V. C. Cheng, K. H. Chan, D. N. Tsang, R. W. Yung, T. K. Ng, and K. Y. Yuen.** 2003. Coronavirus as a possible cause of severe acute respiratory syndrome. Lancet **361:**1319–1325.

20. **Perlman, S., and A. A. Dandekar.** 2005. Immunopathogenesis of coronavirus infections: implications for SARS. Nat. Rev. Immunol. **5:**917–927.
21. **Pyrc, K., B. J. Bosch, B. Berkhout, M. F. Jebbink, R. Dijkman, P. Rottier, and L. van der Hoek.** 2006. Inhibition of human coronavirus NL63 infection at early stages of the replication cycle. Antimicrob. Agents Chemother. **50:**2000–2008.
22. **Ratia, K., S. Pegan, J. Takayama, K. Sleeman, M. Coughlin, S. Baliji, R. Chaudhuri, W. Fu, B. S. Prabhakar, M. E. Johnson, S. C. Baker, A. K. Ghosh, and A. D. Mesecar.** 2008. A noncovalent class of papain-like protease/deubiquitinase inhibitors blocks SARS virus replication. Proc. Natl. Acad. Sci. U. S. A. **105:**16119–16124.
23. **Roberts, A., D. Deming, C. D. Paddock, A. Cheng, B. Yount, L. Vogel, B. D. Herman, T. Sheahan, M. Heise, G. L. Genrich, S. R. Zaki, R. Baric, and K. Subbarao.** 2007. A mouse-adapted SARS-coronavirus causes disease and mortality in BALB/c mice. PLoS Pathog. **3:**e5.
24. **Rockx, B., T. Sheahan, E. Donaldson, J. Harkema, A. Sims, M. Heise, R. Pickles, M. Cameron, D. Kelvin, and R. Baric.** 2007. Synthetic reconstruction of zoonotic and early human severe acute respiratory syndrome coronavirus isolates that produce fatal disease in aged mice. J. Virol. **81:**7410–7423.
25. **Sheahan, T., B. Rockx, E. Donaldson, A. Sims, R. Pickles, D. Corti, and R. Baric.** 2008. Mechanisms of zoonotic severe acute respiratory syndrome coronavirus host range expansion in human airway epithelium. J. Virol. **82:**2274–2285.
26. **Shenoy, S. R., B. R. O'Keefe, A. J. Bolmstedt, L. K. Cartner, and M. R. Boyd.** 2001. Selective interactions of the human immunodeficiency virus-inactivating protein cyanovirin-N with high-mannose oligosaccharides on gp120 and other glycoproteins. J. Pharmacol. Exp. Ther. **297:**704–710.
27. **Sims, A. C., R. S. Baric, B. Yount, S. E. Burkett, P. L. Collins, and R. J. Pickles.** 2005. Severe acute respiratory syndrome coronavirus infection of human ciliated airway epithelia: role of ciliated cells in viral spread in the conducting airways of the lungs. J. Virol. **79:**15511–15524.
28. **Smee, D. F., K. W. Bailey, M. H. Wong, B. R. O'Keefe, K. R. Gustafson, V. P. Mishin, and L. V. Gubareva.** 2008. Treatment of influenza A (H1N1) virus infections in mice and ferrets with cyanovirin-N. Antiviral Res. **80:**266–271.
29. **Tong, T. R.** 2006. SARS coronavirus anti-infectives. Recent Pat. Antiinfect. Drug Discov. **1:**297–308.
30. **Tseng, C. T., C. Huang, P. Newman, N. Wang, K. Narayanan, D. M. Watts, S. Makino, M. M. Packard, S. R. Zaki, T. S. Chan, and C. J. Peters.** 2007. Severe acute respiratory syndrome coronavirus infection of mice transgenic for the human angiotensin-converting enzyme 2 virus receptor. J. Virol. **81:**1162–1173.
31. **van der Hoek, L., K. Pyrc, M. F. Jebbink, W. Vermeulen-Oost, R. J. Berkhout, K. C. Wolthers, P. M. Wertheim-van Dillen, J. Kaandorp, J. Spaargaren, and B. Berkhout.** 2004. Identification of a new human coronavirus. Nat. Med. **10:**368–373.
32. **van der Meer, F. J., C. A. de Haan, N. M. Schuurman, B. J. Haijema, W. J. Peumans, E. J. Van Damme, P. L. Delputte, J. Balzarini, and H. F. Egberink.** 2007. Antiviral activity of carbohydrate-binding agents against Nidovirales in cell culture. Antiviral Res. **76:**21–29.
33. **van der Meer, F. J., C. A. de Haan, N. M. Schuurman, B. J. Haijema, M. H. Verheije, B. J. Bosch, J. Balzarini, and H. F. Egberink.** 2007. The carbohydrate-binding plant lectins and the non-peptidic antibiotic pradimicin A target the glycans of the coronavirus envelope glycoproteins. J. Antimicrob. Chemother. **60:**741–749.
34. **Winter, C., G. Herrler, and U. Neumann.** 2008. Infection of the tracheal epithelium by infectious bronchitis virus is sialic acid dependent. Microbes Infect. **10:**367–373.
35. **Wohlford-Lenane, C. L., D. K. Meyerholz, S. Perlman, H. Zhou, D. Tran, M. E. Selsted, and P. B. McCray, Jr.** 2009. Rhesus theta-defensin prevents death in a mouse model of severe acute respiratory syndrome coronavirus pulmonary disease. J. Virol. **83:**11385–11390.
36. **Woo, P. C., S. K. Lau, C. M. Chu, K. H. Chan, H. W. Tsoi, Y. Huang, B. H. Wong, R. W. Poon, J. J. Cai, W. K. Luk, L. L. Poon, S. S. Wong, Y. Guan, J. S. Peiris, and K. Y. Yuen.** 2005. Characterization and complete genome sequence of a novel coronavirus, coronavirus HKU1, from patients with pneumonia. J. Virol. **79:**884–895.
37. **Ziolkowska, N. E., B. R. O'Keefe, T. Mori, C. Zhu, B. Giomarelli, F. Vojdani, K. E. Palmer, J. B. McMahon, and A. Wlodawer.** 2006. Domain-swapped structure of the potent antiviral protein griffithsin and its mode of carbohydrate binding. Structure **14:**1127–1135.
38. **Ziolkowska, N. E., S. R. Shenoy, B. R. O'Keefe, J. B. McMahon, K. E. Palmer, R. A. Dwek, M. R. Wormald, and A. Wlodawer.** 2007. Crystallographic, thermodynamic, and molecular modeling studies of the mode of binding of oligosaccharides to the potent antiviral protein griffithsin. Proteins **67:**661–670.

HIV-1 Neutralization Profile and Plant-based Recombinant Expression of Actinohivin, an Env Glycan-specific Lectin Devoid of T-cell Mitogenic Activity

Running header: Anti-HIV-1 activity and plant-based expression of actinohivin

Nobuyuki Matoba[1, 2, *], Adam Husk[1], Brian Barnett[1], Michelle Pickel[3], Charles J. Arntzen[3], David C. Montefiori[4], Atsushi Takahashi[5], Kazunobu Tanno[6], Satoshi Omura[7], Huyen Cao[8], Jason Mooney[8], Carl V. Hanson[8], and Haruo Tanaka[4, 5]

[1] Owensboro Cancer Research Program, James Graham Brown Cancer Center, Kentucky 42303, and [2] Department of Pharmacology & Toxicology, University of Louisville School of Medicine, Louisville, Kentucky 40292;

[3] Center for Infectious Diseases and Vaccinology at the Biodesign Institute, P.O. Box 874501, Arizona State University, Tempe, Arizona 85287- 4501;

[4] Department of Surgery, Duke University Medical Center, Durham, North Carolina 27710;

[5] Faculty of Pharmacy and College of Science and Engineering, Iwaki Meisei University, Iwaki, Fukushima 970-8551, Japan;

[6] KIIM Pharmaceutical Laboratories, Inc., Iwaki, Fukushima 970-8551, Japan;

[7] Kitasato Institute for Lifescience, Kitasato University, Minato-ku, Tokyo 108-8641, Japan;

[8]California Department of Public Health, Richmond, California 94804

*Correspondence to: Nobuyuki Matoba

Owensboro Cancer Research Program, 1020 Breckenridge Street, Suite 201, Owensboro, KY 42303. Phone: 270-691-5955; Fax: 270-685-5684; Email: n.matoba@louisville.edu

Abstract

The actinomycete-derived lectin actinohivin (AH) is highly specific to a cluster of high-mannose-type glycans uniquely found on the HIV-1 envelope (Env). Two validated *in vitro* assays based on human peripheral blood mononuclear cell (hPBMC) infection with primary isolates and TZM-bl cell infection with Env-pseudotyped viruses were employed to characterize AH's anti-HIV-1 activity. In hPMBCs, AH exhibited nanomolar neutralizing activity against primary viruses with diverse cellular tropisms, but did not cause mitogenicity or cytotoxicity often associated with other anti-HIV lectins. In the TZM-bl-based assay, AH showed broad anti-HIV-1 activity against mucosally transmitting strains of clades B and C, but not clade A. Correlation analysis suggested that HIV-1's AH susceptibility is linked to the *N*-glycans at the Env C2 and V4 regions. To facilitate our further investigation of AH, we evaluated tobacco mosaic virus (TMV)-based expression of recombinant (r)AH in *Nicotiana benthamiana* plants. Biochemical analysis and a syncytium formation assay demonstrated high-level expression of functional rAH within 6 days. Taken together, our study revealed AH's cross-clade anti-HIV-1 activity, apparent lack of side effects common to lectins, and robust producibility using plant biotechnology. These findings justify further efforts to develop rAH toward candidate HIV-1 microbicides.

Introduction

For nearly 30 years, HIV has posed serious global health concerns. Millions of new HIV infections are reported every year worldwide, mainly in developing regions where the availability of antiretroviral drug therapies is extremely limited. As a result, AIDS is among the leading causes of death in these regions (1). The majority of infections are established via heterosexual transmission and condom use is currently the only available means to directly block this route of infection. As such, the need is urgent for woman-controlled, safe, effective, and inexpensive topical microbicides, until prophylaxis through vaccination becomes globally available (2, 3).

Current candidate microbicides under development encompass chemical and physical agents as well as biologicals, including virion-inactivating agents, entry/fusion inhibitors, reverse transcriptase inhibitors, and others (www.microbicide.org). At this point, it is not known which type of anti-HIV agents will be most effective as topical microbicides; blocking of HIV-1 mucosal transmission may require combinations of multiple agents (4, 5). Therefore, to broaden the options for different combinations in HIV-1 microbicide development, it is important to expand the candidate portfolio in each category of possible microbicide components.

The envelope (Env) gp120 is heavily glycosylated with *N*-linked glycans (NLGs), which generally account for more than half of the protein's molecular mass (6). Of these, HMGs represent a major class. Because the Env glycans play critical roles in broad aspects of the viral life cycle ranging from Env folding in host cells to viral transmission and immune escape (7), they constitute an attractive target for entry/fusion inhibitor-based microbicide development.

Therefore, lectins have attracted considerable attention. Various naturally occurring lectins have been shown to possess anti-HIV activities. Examples include algae-derived cyanovirin-N (CV-N) and griffithsin (GRFT) as well as plant-derived concanavalin A (Con A) and snowdrop

lectin, among others (reviewed in: (7)). More recently, a Jacalin-related lectin isolated from the banana fruit was shown to potently inhibit HIV-1 entry into target cells (8). Although conceptually not a lectin, the human monoclonal antibody (mAb) 2G12 specifically binds to gp120 HMGs and is a member of the very few broadly neutralizing mAbs isolated to date (9, 10).

AH was isolated from the actinomycete strain *Longispora albida* K97-0003^T based on the inhibitory activity in a syncytium formation assay (11). Unlike other anti-HIV lectins reported to date (7), AH specifically recognizes a cluster of multiple HMGs via its three sugar-binding sites (12, 13). Because clustering HMGs is a unique feature of Env glycans and not usually found on host human proteins (14), AH is hypothesized to be a superior anti-HIV-1 lectin with exquisite specificity to the virus; hence, it may be devoid of unfavorable biological impacts in humans.

In spite of the detailed studies in AH's carbohydrate-binding specificity (12, 13, 15), limited investigation has been reported with regard to the protein's anti-HIV activity in a syncytium formation assay and in a multinuclear-activation-of-galactosidase-indicator (MAGI) assay (15). Because there is currently no *in vitro* assay that can accurately predict *in vivo* efficacy of a candidate anti-HIV-1 agent, it is important to evaluate the activity of a potential anti-HIV compound in multiple *in vitro* assay systems that closely simulate the *in vivo* situation and analyze anti-HIV-1 activity in a broad-spectrum of clinically relevant viruses from different clades (16). Another important factor for a protein-based microbicide candidate is the development of an efficient, cost-effective recombinant expression system that is compatible with extensive preclinical and clinical studies, global distribution, and molecular design for the construction of stronger and/or safer derivatives.

Thus, the primary objectives of our study were to reveal AH's anti-HIV-1 potential in validated *in vitro* neutralization assay systems and to develop a robust expression platform for rAH. To this end, we employed a human peripheral blood mononuclear cell (hPBMC)-based

neutralization assay using primary HIV-1 isolates and a reporter gene expressing TZM-bl cell-based neutralization assay using Env-pseudotyped viruses from diverse clades, including clinically relevant C-C chemokine receptor 5-tropic (R5) HIV-1 strains. For recombinant expression of AH, we tested a rapid and robust tobacco mosaic virus (TMV)-based expression system in *Nicotiana benthamiana* plants. Thus, we provide data implicating the feasibilities of AH in terms of its efficacy and production viability. In addition, we performed a preliminary analysis of AH to screen for potential side effects commonly noted with antiviral lectins, i.e., cytotoxicity and mitogenic activity in hPBMCs.

Materials and Methods

The hPBMC-based primary HIV-1 neutralization assay

The hPBMCs used in the HIV neutralization assay and proliferation analysis described below were purchased from the local blood center as an otherwise-discarded by-product of unsolicited blood donations. No information about identity of the donors was available to the investigators.

The assay was conducted essentially as described in D'Souza et al. (17) and Mascola et al. (18). Accordingly, the infectious viruses were produced in hPBMCs. The hPBMCs were prepared from buffy coats using Lymphocyte Separation Medium (LSM; Cappel, Aurora, OH). To reduce variation of data from different cell preparations, the cell samples from four different donors were pooled and frozen so that a series of experiments was performed using the same hPBMC pool. An inoculum of 100 50% tissue culture infectious dose ($TCID_{50}$) of HIV-1 was mixed with test samples and incubated for 1 h at 37°C. Next, $3x10^5$ of phytohemagglutinin (PHA)-stimulated hPBMCs were added and incubated for 72 h, and washed to remove residual

virus/sample inoculum. After an additional 24-h incubation, cells were lysed and p24 was quantified using a Beckman Coulter (Fullerton, CA) HIV-1 p24 Antigen Assay Research Component Kit. Neutralization was defined as the percent reduction in the amount of p24 detected with the test samples as compared to control. Inhibitory concentrations of 50% (IC_{50}) were determined via nonlinear regression analysis using the GraphPad Prism 5 (GraphPad Software, La Jolla, CA). Samples were analyzed in quadruplicate. In each assay, anti-clusters of differentiation antigen 4 (CD4) mAb B4 was used as a positive control (19). To minimize inter-assay variations of neutralization activity, sample IC_{50}s were normalized using B4 IC_{50} values obtained in each assay.

Cytotoxicity and mitogenic activity in hPBMCs

For cytotoxicity analysis, the CytoTox-ONE™ Homogeneous Membrane Integrity Assay Kit (Promega, Madison, WI) was used to estimate cell viability. hPBMCs were prepared as described above. A test sample was mixed with 2.5 $x10^5$ hPBMCs and incubated for 6 h at 37°C. Cell viability treated with test samples was calculated by relative lactate dehydrogenase activity in culture medium of that in lysed cell controls.

The proliferative activity of AH in hPBMCs was analyzed by carboxyfluorescein succinimidyl ester (CFSE) staining as described in Elrefaei et al. (20), using the Molecular Probes CellTrace Kit (Invitrogen, Eugene, OR). One million hPBMCs were labeled with 2 µM CFSE and cultured in the presence of a test sample (12.5 µg/ml AH, 1 µg/ml staphylococcal enterotoxin B [SEB, a positive control T cell stimulant (21)], or media alone [negative control]) for 5 days at 37°C in a CO_2 incubator. Cells were stained with BD Pharmingen anti-human CD4 phycoerythrin (PE), anti-human CD8 peridinin chlorophyll protein with a cyanine dye (PerCP-Cy5.5), and anti-human CD3 allophycocyanin (APC; BD Biosciences, San Jose, CA), and analyzed by an LSR II

cell analyzer (BD Biosciences) and FlowJo software (TreeStar, Ashland, OR). Samples were first gated on viable lymphocyte population, and percentage of proliferating cells was determined by measuring the extent of CFSE dilution. The analysis was independently performed three times, using hPBMCs from three different donors.

The TZM-bl-based Env-pseudotyped HIV-1 neutralization assay

The antiviral activity of AH was assessed based on a reduction in luciferase reporter gene expression after infection of TZM-bl cells with Env-pseudotyped viruses. The assay was performed as described elsewhere (22), except that diethylaminoethyl cellulose dextran was excluded upon infection. Antiviral activity was expressed as an IC_{50} value, which is the sample concentration giving 50% of relative luminescence units (RLUs) compared with those of virus control after subtraction of background RLUs. Env-pseudotyped viruses were prepared by co-transfection of 293T/17 cells with various *env*-expressing plasmids and an *env*-deficient HIV-1 backbone vector (pSG3ΔEnv) and were titrated in TZM-bl cells as previously described (22) to determine $TCID_{50}$. The Genbank accession numbers of the viruses used in the assay are shown in Table 2. The broadly neutralizing mAbs b12, 2G12, 2F5 and 4E10, as well as soluble CD4 were used as positive controls. Two-hundred $TCID_{50}$ of pseudoviruses were used for the neutralization assay. Samples and the virus were mixed and incubated for 1 h at 37°C, to which 10^4 cells/well of TZM-bl cells were added and incubated for 72 h. Luciferase activity was measured using the Britelite Plus Reagent (PerkinElmer, Waltham, MA).

Correlation analysis

Env potential NLG sites were determined based on sequons (Asn-X-Thr/Ser-Y, where X and Y are any aa except for Pro) using in Env sequences of viruses tested in the TZM-bl-based assay (provided in Genbank) and the online tool N-Glycosite at Los Alamos HIV Database (http://www.hiv.lanl.gov/content/sequence/GLYCOSITE/glycosite) (23). The correlation between the IC_{50}s and the number of sequons at whole or the selected Env region was analyzed using the non-parametric Spearman's correlation coefficient in the GraphPad Prism 5 software. To allow this analysis using all the viruses tested in the TZM-bl-based assay, any IC_{50} values greater than the highest concentration tested were arbitrary approximated to the next two-fold dilution step (i.e., 50 µg/ml for experimental IC_{50}s >25 µg/ml).

rAH expression in *N. benthamiana*

A "deconstructed" TMV replicon system (magnICON; Icon Genetics GmbH, Halle/Saale, Germany) was used (24, 25) to express rAH in *N. benthamiana*. The native *ath* gene (Genbank accession no. AB032371) was sub-cloned into the gene expression module pICH11599 using Nco I and Sac I restriction sites to form pNM86. The three component plasmids (pNM86, pICH20111, and pICH14011) were each transferred into the *Agrobacterium tumefaciens* strain GV3101 by electroporation. Bacteria were resuspended in an infiltration buffer (10 mM 2-(*N*-morpholino)ethanesulphonic acid [MES], 10 mM $MgSO_4$, pH 5.5). Equal portions of the three bacteria were then mixed to give an optical density at 600 nm (OD600) of 0.1. *N. benthamiana* plants were grown at 27°C and 55 – 65% humidity for 4 weeks under an 18 h-light/6 h-dark cycle. Forty-eight h before inoculation, plants were moved to an incubator set at 22°C and 55 – 65% humidity with the same lighting cycle. The bacteria suspension was infiltrated into leaves by application of a vacuum for 2 min at 25 inches Hg using a vacuum pump. After infiltration, plants were placed in the incubator set at 22°C and kept in darkness for 16 h. Subsequently, the

incubator was set to a normal 18 h-light/6 h-dark cycle. At 4 to 6 days post infiltration (dpi), infected leaves were harvested and examined for rAH expression as described below.

Detection of rAH

Expression of rAH was analyzed by sodium dodecyl sulfate-polyacrylamide gel electrophoresis (SDS-PAGE) and western blotting. Leaf materials were extracted with 5 v/w of SDS extraction buffer (50 mM Tris-HCl [pH 6.8], 2% SDS, 0.003% bromophenol blue, 10% glycerol). After electrophoresis, gels were stained with Coomassie Brilliant Blue, or the resolved proteins were electro-transferred to a poly (vinylidene difluoride) membrane. Blots were probed with rabbit anti-AH antiserum (1:5,000) followed by horseradish peroxidase (HRP)-conjugated goat anti-rabbit immunoglobulin (Ig)G (1:10,000; Santa Cruz Biotechnology, Santa Cruz, CA), which were then detected using a chemiluminescence luminol reagent (Santa Cruz Biotechnology).

The amounts of rAH in extract were quantified by gp120-captured enzyme-linked immunosorbent assay (gp120-ELISA). ELISA plates were coated with 0.3 µg/ml of HIV-1 gp120 CM Env protein (National Institute of Health AIDS Research and Reference Reagent Program [NIH ARRRP], Washington, D.C.) and blocked with blocking buffer (phosphate-buffered saline [PBS], pH7.2, 0.05% Tween-20, 5% [w/v] non-fat dry milk). Serially diluted extract samples were applied onto the plates and incubated for 1 hr at 37ºC. The gp120-bound rAH was detected by rabbit anti-AH antiserum (1:3,000) followed by HRP-conjugated goat anti-rabbit IgG (1:10,000). A tetramethylbenzidine substrate (BioFX Laboratories, Owings Mills, MD) was used for detection; absorbance at 450 nm was measured with a plate reader (Beckman Coulter). A standard curve was created for each plate using standard AH (5 – 300 ng/ml; purified from

original actinomycete culture), with which the amounts of rAH in samples were calculated using the SoftMax Pro software (Molecular Devices, Sunnyvale, CA).

Syncytium Formation Assay

The assay was performed as previously described, using HeLa/env/tat and HeLa/CD4/lacZ cell lines (26). To prepare leaf extract samples for analysis, leaf materials were homogenized in 5 v/w of extraction buffer 1 (PBS, pH7.4, 20 mM ascorbic acid, 10 mM sodium metabisulfite) and centrifuged. Most (>99%) of the total gp120-binding rAH was retained in the insoluble pellet fraction. The pellet was re-extracted with extraction buffer 2 (50 mM glycine, pH2.5, 20 mM ascorbic acid, 10 mM sodium metabisulfite, 6 M guanidine HCl). The extract was clarified by centrifugation and dialyzed against 50 mM glycine (pH 2.5). The dialyzed sample was centrifuged to remove insoluble materials and concentrated using a centrifugal concentrator (3.5 kDa molecular weight cut-off). The amount of rAH in each fraction was quantified by gp120-ELISA, as described above. Typically, in the dialyzed sample we obtained ~25 μg of rAH from one g of leaf material.

For a quantitative assay, serially diluted samples and 9×10^3 cells/well of HeLa/env/tat and HeLa/CD4/LacZ cells were mixed in GIBCO Dulbecco's modified Eagle's medium (DMEM; Invitrogen, Carlsbad, CA) containing 10% fetal bovine serum, 1% penicillin/streptomycin and 100 μg/ml kanamycin on a 96-well plate and incubated for 18 h at 37°C in a CO_2 incubator. Cells were washed and lysed with 0.05% Triton X-100. To quantify syncytia, a developing reagent (60mM Na_2HPO_4, 40 mM NaH_2PO_4, 10 mM KCl, 1 mM $MgSO_4$, 50 mM 2-mercaptoethanol, 0.8 mg/mL ortho-Nitrophenyl-β-galactoside) was added and incubated at room temperature for 2 to 4 h. After stopping the reaction with 2M Na_2CO_3, the OD_{450} was read.

For staining of syncytia, HeLa/env/tat and HeLa/CD4/LacZ (10^5 cells each/well) with or without a test sample were incubated on an 8-well microscope slide (Nalge Nunc International, Rochester, NY) for 18 h at 37°C. Cells were washed with PBS, and fixed with 4% paraformaldehyde. Syncytia were stained with 5-bromo-4-chloro-3-indolyl-β-D-galactopyranoside (X-gal) staining solution (25ml PBS, pH 7.4, 2 μg/ml $MgCl_2$, 1.64 mg/ml potassium ferricyanide, 2.12 mg/ml potassium ferrocyanide, 1mg/ml X-gal) for 18 h at 37°C and observed under an optical microscope.

Results

AH inhibits hPBMC infection by primary HIV-1 isolates. Given that clustering HMGs is a conserved feature of the HIV-1 Env, broad anti-HIV-1 activity has been suggested for the HMG-specific lectin AH. To prove this concept in an assay system simulating the physiological conditions, we performed a hPBMC-based neutralization assay using primary HIV-1 isolates (17, 18). Viruses with diverse cellular tropisms were tested, i.e., an R5 B clade (SF162), an R5 C clade (ZA/97/009), a chemokine (C-X-C motif) receptor 4-tropic (X4) B clade (HT/92/599), and a dual-tropic R5X4 B clade (BZ167). The p24 production in the cells was quantified to monitor HIV-1 infectivity. As shown in Figure 1A, AH neutralized all the viruses with IC_{50}s within the nanomolar range (1 μg/ml of AH corresponds to 80 nM). Among the four primary isolates tested, the R5-type C clade virus showed the highest susceptibility to AH (IC_{50} = 0.12 μg/ml or 9.6 nM and IC_{90} = 12.10 μg/ml or 968 nM) whereas the X4 B clade virus was relatively resistant (IC_{50} = 2.68 μg/ml or 224 nM and IC_{90} = 29.67 μg/ml or 2,370 nM). These results are congruent with the previous findings in a surrogate MAGI assay, where AH exhibited antiviral activity at the nanomolar dose range (IC_{50}s = 2 – 110 nM) against three laboratory-adapted T- and M-tropic

strains (IIIB, NL4-3, and JR-CFS) and one T-tropic primary isolate (O18A) (15). Meanwhile, AH did not show any cytotoxicity in hPBMCs at the highest concentration tested (50 μg/ml or 4 μM), indicating that the reduction of p24 production in the assay was not due to cytotoxicity (Fig. 1B). Taken together, these results demonstrated that AH can inhibit the infection of hPBMCs by primary HIV-1 strains irrespective of cellular tropism, which directly suggests the possibility of the protein's *in vivo* efficacy.

AH does not induce hPBMC proliferation at a dose exerting strong anti-HIV-1 activity. Many lectins are known to exhibit various biological effects on human cells via their specific carbohydrate binding. For example, Con A and PHA are well-known mitogens in human T cells (27). The banana-derived lectin entry inhibitor BanLec effectively proliferated $CD3^+$, $CD4^+$ and $CD8^+$ populations in hPBMCs at 2 μg/ml (corresponding to ~67 nM as a natural dimer form) (28). Furthermore, strong mitogenic activity and cytotoxicity in hPBMCs was observed for CV-N, which has been one of the most studied HMG-specific anti-HIV-1 lectins to date (29, 30). Because hPBMC mitogenicity may lead to the disastrous side effect of *enhanced* HIV-1 infectivity in these cells (29), it is imperative to demonstrate that the anti-HIV-1 effect of a candidate microbicide is not accompanied by mitogenic activity in these cells. Therefore, we tested the proliferation potential of hPBMCs upon exposure to AH. As shown in Figure 2, AH at 1 μM (or 12.5 μg/ml) did not show any sign of proliferative activity either in a whole $CD3^+$ T cell population or in $CD4^+$ or $CD8^+$ cells after prolonged incubation (for 5 days) with AH. These results are in sharp contrast to the protein's nanomolar anti-HIV-1 activity in the hPBMC-based neutralization assay, where the same dose exerted a prominent HIV-1 neutralization effect against primary isolates (Fig. 1A). Coupled with the data showing AH's lack of cytotoxicity up to 4 μM (see Fig. 1B), it is suggested that AH anti-HIV-1 activity is not associated with some of the major common side effects noted with other antiviral lectins.

Broad-spectrum anti-HIV-1 activity of AH against R5-type viruses. To extend our examination on the breadth of AH's anti-HIV-1 activity, we performed a reporter gene expression TZM-bl-based neutralization assay using Env-pseudotyped viruses (22). We included multiple R5 A, B and C clade viruses in the analysis because: 1) R5 viruses are transmitted predominantly during the course of HIV-1 transmission (31, 32) and are therefore particularly important from an HIV-1 microbicide standpoint; and 2) these three clades represent more than 70% of the viruses currently circulating in the world (33, 34). Table 1 shows IC_{50}s of AH against clade A, B, and C isolates of AH and the HMG-specific broadly neutralizing mAb 2G12. AH showed broad anti-HIV-1 activity that was similar overall to that of 2G12, aside from a few exceptions. Among the viruses tested, ZM109F.PB4 (R5 C clade) and all the four A clade viruses showed IC_{50}s of over 25 μg/ml for both AH and 2G12. These results may indicate that clade A viruses are generally highly resistant to the two HMG-specific anti-HIV proteins compared to other subtypes. By contrast, the notable difference between AH and 2G12 was seen with other viruses. SF162 (B clade R5) and 6535.3 (B clade R5) showed complete resistance to AH (IC_{50}s >25 μg/ml) but not to 2G12, while RHPA4259.7 (B clade R5), MW965.26 (C clade R5), and ZM214M.PL15 (C clade R5) were susceptible to AH but resistant to 2G12. These results indicate that the Env glycan target and/or anti-HIV mode are different between these two proteins. Of interest is the fact that SF162, which showed relatively high susceptibility to AH in the hPBMC-based assay (IC_{50} = 0.48 μg/ml, Fig. 1), was highly resistant to this protein in the TZM-bl-based neutralization assay. On the other hand, the dual-tropic B clade BZ167, another virus strain used in both assay formats, showed similar sensitivity to AH (IC_{50}s at 0.8 μg/ml in the hPBMC-based assay vs. 2.9 μg/ml in the TZM-bl-based assay).

To partly discern whether AH's anti-HIV-1 effect is associated with a particular Env NLG pattern, the IC_{50}s obtained in the TZM-bl-based neutralization assay were plotted against the number of potential *N*-glycosylation sites on Env (Fig. 3). There was no clear correlation

between AH-susceptibility and the number of sequons on whole Env or V regions. On the contrary, a relative correlation was observed between AH susceptibility and sequons at entire C regions (Spearman correlation coefficient [r] = -0.40, p = 0.084). Site-specific analysis revealed that sequons at the C2 segment alone have a significant correlation (r = -0.51, p = 0.020). Notably, this correlation became even more apparent when sequons at the C2 and V4 regions were combined (r = -0.65, p = 0.002), even though V4 sequons alone were not strong enough to show a significant correlation with AH-susceptibility (p = 0.176). Throughout the Envs from all the viruses analyzed, there was no significant change in the number of sequons in C1, C4, C5, V3, or gp41. Relatively high degrees of numerical variations were observed in V1/V2, V5, and C3 regions, but no correlation with AH susceptibility was detected in these regions (data not shown). Taken together, these results suggest that NLGs at C2 and V4 may constitute the sole and/or critical targets of AH. In Figure 4, we compared Env NLG positions of the highly susceptible viruses (R5 B clade SS1196.1 and R5 C clade TV1.21) and resistant strains (R5 C clade ZM109F.PB4 and R5 A clade Q259.d2.17). It was suggested that clustering NLGs at the middle and C terminal region of C2 as well as in V4 may play an important role in AH's anti-HIV-1 activity.

For a comparison, we also performed the same analysis with 2G12. It was revealed that 2G12 susceptibility showed a statistically significant correlation with the total number of sequons located at C2, C3 and V4 (r = -0.52, p = 0.034) and with V4 sequons alone (r = -0.53, p = 0.028), but not with any other Env regions (data not shown). These results correspond well with previous mutagenesis and crystallographic studies that have defined the Env NLGs targeted by 2G12 (10, 35), thus arguing for the present approach to predict AH's potential binding target(s).

Expression of rAH in *N. benthamiana* using a modified TMV vector. Next, we focused on the development of an efficient rAH expression system to facilitate the production and molecular engineering of the protein. For this purpose, a modified TMV-based expression

system was employed (24, 25). Under our normal plant growth conditions at 27°C, severe necrosis emerged in the infiltrated leaves at 4 to 5 dpi. However, the necrosis was significantly reduced by lowering the plant cultivation temperature by 5°C, i.e., to 22°C (Fig. 4A). The expression level of rAH did not change by this modification, according to gp120-ELISA (data not shown). As shown in Figure 4B, the expression of rAH (Mw: 12.5 KDa) was clearly detected at 5 dpi on an SDS-PAGE gel. Western blot analysis using polyclonal anti-AH Abs further confirmed the expression (Fig. 4B). Interestingly, however, apparent oligomers (dimer, trimer, etc) and aggregates were detected along with the monomeric 12.5 kDa protein (Fig. 4B). No oligomer formation has previously been noted for the original actinomycete-derived AH (11, 13), although an apparent dimer was observed in *E. coli*-expressed rAH (36) and a minor amount of dimers exists in a purified actinomycete-derived AH sample (Matoba et al., unpublished observation). Therefore, the oligomer/aggregate formation is unique to the TMV-based expression. The gp120-ELISA of the leaf extract revealed that the expression of rAH peaked at 6 dpi, with expression levels ranging from 20 to 120 mg per kg of fresh leaf material (data not shown), which generally agrees with the intensity of the band in SDS-PAGE in Figure 4B.

The efficient recovery of the gp120-binding fraction of rAH from the leaf required an acidic extraction buffer containing a chaotropic agent such as urea or guanidine HCl. After removing the denaturant by dialysis, however, rAH remained soluble and was largely devoid of high-order oligomers (Fig. 4B, lane 7). The soluble plant-expressed rAH strongly bound to gp120 (Fig. 5A). To further demonstrate plant-expressed rAH's functional integrity, we performed a reporter gene expression syncytium formation assay using cells expressing human CD4 and HIV-1 Env. As seen in Figure 5B, the X-gal staining of the cells clearly shows that plant-expressed rAH (Fig. 5B-d), but not a reference control prepared from a non-infiltrated leaf sample (Fig. 5B-b), inhibited the formation of syncytia. No inhibition was observed with a sample from GFP-expressing leaves obtained by the same TMV-based vector (data not shown). This observation

was further confirmed by a quantitative analysis. Thus, plant-expressed rAH dose-dependently and significantly inhibited the syncytia compared to a control leaf sample (Fig. 5C). According to the gp120-ELISA in Fig. 5A, a 1/20-diluted rAH sample contained 322 nM of the protein (corresponding to the far-right bar in Fig. 5C). The results were in good agreement with the syncytium-inhibitory pattern of the original AH sample (data not shown), indicating the integrity of the plant-expressed protein. Taken together, these results demonstrate that plants can serve as a new recombinant expression platform for AH and that plant-expressed rAH is functionally active.

Discussion

HIV/AIDS is a serious global public health concern. In the most pandemic sub-Saharan African countries, heterosexual exposure constitutes the major route of HIV-1 transmission, with half of the new infections occurring among women (1). Although condom use and male circumcision can significantly reduce the chance of HIV-1 sexual transmission, there is no direct countermeasure currently available at women's disposal (1). Therefore, the development of a woman-controlled microbicide is urgently needed for the control of the pandemic. Three key factors are proposed for candidate microbicides to move from the preclinical to clinical phase, i.e., efficacy, safety, and economical viability (3). We have therefore initiated our investigation on the feasibility of AH in these aspects.

AH is an actinomycete-derived anti-HIV protein that has high specificity to HMG clusters on Envs. In the two *in vitro* HIV-1 neutralization assays performed here, we obtained several key advances in understanding the anti-HIV-1 activity profile of AH.

First, AH's anti-HIV-1 effect was demonstrated in a hPBMC-based assay using primary isolates and in a TZM-bl-based assay using Env-pseudotyped viruses of clinically-relevant strains from major clades. These two *in vitro* assay formats are currently recommended for evaluating the anti-HIV-1 activity of neutralizing Abs, hence entry/fusion inhibitors, to best predict their *in vivo* antiviral efficacies (37). In both assay systems AH exhibited clear anti-HIV-1 effects against many clinically relevant viruses, including those of the mucosally transmitted R5-type, at similar activity dose ranges. Consequently, it is strongly argued that AH is a broadly neutralizing anti-HIV-1 lectin that could potentially blunt mucosal HIV-1 transmission of primary R5 viruses. A future study will test the anti-HIV-1 effect in systems more closely simulating the physiological conditions in the vagina, e.g., in the presence of seminal plasma and under a pH transition that takes place during the coital event (38). Sustained efficacy under these conditions, along with safety (as discussed below), are prerequisites for any microbicide candidate.

While AH's anti-HIV-1 effects in the hPBMC-based- and TZM-bl-based neutralization assays fell into a similar range, there was a significant difference in the sensitivity of the B clade SF162 to AH between the two systems (see Fig. 1 and Table 1). Multiple studies have reported similar discrepancies in inhibitory patterns of neutralizing Abs between the two assay systems (16, 37). In our case, the conflicting result may be a reflection of the phenotypic difference in viruses produced in these assays, i.e., the primary isolate produced in hPBMCs versus the Env-pseudotyped virus produced in 293T cells. It has been shown that the *N*-glycan structure of viral glycoproteins can vary depending on the cell type in which the virus is produced (14, 39, 40). Because AH targets Env HMGs, it is conceivable that viruses harboring more HMGs on their Envs would be more susceptible to the protein. Thus, although there is no direct information as to the glycan profiles of SF162 Envs produced in hPBMCs and 293T cells, the higher AH sensitivity of the hPBMC-produced virus may be explained by the higher number of HMGs on the Env. Alternatively, a potential difference in the Env density on the viruses used in the two

different systems may account for the discrepancy in viral AH sensitivity, as has been reported (41, 42). In any event, the above may imply that a future efficacy study of AH or other relevant anti-HIV-1 agents should include testing of viruses present in semen (43, 44).

Second, we uncovered the breadth of AH's anti-HIV-1 effect in the TZM-bl-based neutralization assay. It was revealed that AH possesses anti-HIV-1 activity against many clinically relevant R5 viruses, having the neutralization breadth similar to that of the HMG-targeting broadly neutralizing mAb 2G12. This is not surprising because both 2G12 and AH recognize the Manα1-2Man moiety of HMGs (9, 10, 13, 35). However, a few discrepancies in the neutralization patterns between 2G12 and AH indicate that their target HMGs are not identical (discussed later). AH may generally be more effective against R5 C clade viruses than 2G12, as the former neutralized four viruses while the latter inhibited only two out of the five viruses tested at lower than 25 μg/ml (Table 1). This points to an advantage of AH because the C clade is highly prevalent in epidemic regions where over 80% of total global HIV-1 infections occur (33, 34), although analysis must be expanded to validate this concept. On the other hand, both AH and 2G12 showed lack of efficacy to all the four A clade viruses. Interestingly, relative resistance of A clade viruses has previously been observed for another potent mannose-specific anti-HIV-1 lectin, GRFT (45). These results may indicate the general resistance of A clade viruses to HMG-targeting HIV-1 inhibitors and imply a potential weakness for this class of anti-HIV agent. Alternatively, this warrants investigation of more in depth clade-specific analysis and identification of a different type of anti-HIV agent that can supplement AH or other HMG-targeting HIV-1 inhibitors toward an effective combination microbicide strategy.

Third, correlation analysis between AH susceptibility and Env NLG profiles suggested that several NLGs might be targeted by AH. These glycans tend to cluster at the middle and at the C-terminal region of C2 and at V4 (Fig. 4). A recent crystallographic analysis indicated that AH possesses three carbohydrate-binding sites and that each of these appeared to accommodate a

couple of Manα1-2Man moieties from the D1 and D3 arm of a single HMG (13). Our results suggest that NLGs at the C2 and V4 regions may comprise a set of HMGs recognized by AH's three sugar binding sites. This notion is supported in part by the previous studies showing that NLGs at these locations tend to contain more HMGs than other regions (46-48). Obviously, further studies are needed to demonstrate AH's target Env NLGs, e.g., crystallography of an AH-gp120 complex, and analysis of escape and mutant viruses displaying modified Env NLG patterns. Such studies will also aid the development of potent AH analogues and are ongoing in our laboratories.

AH is similar to CV-N in that both lectins recognize the Manα1-2Man structure of HMGs and thereby exert anti-HIV-1 activity, although the former relies on high-avidity interaction with multiple HMGs while the latter is specific to a single HMG (13, 49, 50). CV-N is a leading lectin-based microbicide candidate that has shown promising results in macaque challenge studies (51, 52) and in a human cervical explant infection model (53). However, recent studies have shown that CV-N possesses cytotoxicity and mitogenic activity with pro-inflammatory responses in hPBMCs at nanomolar concentrations, which are very close to the protein's antiviral dose range (29, 30). These deleterious and pro-infective actions have raised a serious concern for CV-N's candidacy toward microbicide use. Indeed, such activities are common features of lectins (with a few notable exceptions, e.g., GRFT (45)), necessitating careful examination of lectin-based HIV-1 inhibitors in these aspects. In spite of the similarity between CV-N and AH in sugar binding specificity, our results demonstrated that AH is devoid of cytotoxicity or mitogenic activity in hPBMCs at concentrations where the protein exerts potent anti-HIV-1 effects. More thorough analyses, including inflammatory endpoints and immunogenicity, must be performed for higher doses of AH to conclude the protein's safety. Nevertheless, when combined with AH's specificity to HMG clusters usually not found on host human proteins and preliminary results showing the lack of toxicity in a rabbit vaginal irritation assay with 0.1% AH solution (Tanaka et

al. manuscript in preparation), our results provide a reasonable foundation supporting the protein's safety.

Microbicides will be required in massive amounts at low costs, considering the application frequency and estimated target population of those millions living in developing regions where HIV-1 infections are most prevalent. Accordingly, a key factor for the success of protein-based HIV-1 microbicides is the establishment of a scalable and cost-effective recombinant expression system; however conventional closed cell culture-based systems may not be able to meet these requirements (54). Plants have recently emerged as an alternative recombinant expression system that has the potential to mass produce foreign proteins at substantially low costs (55, 56). In particular, the advent of recombinant plant virus vector systems enabled rapid and high-level expression of foreign proteins in plants. In the present study, we showed that rAH expressed via a TMV-based system can bind to gp120 and inhibit syncytia mediated by the Env-CD4 interaction, which demonstrates the protein's functional integrity. Although there is room for improvement (e.g., reducing *in planta* aggregate formation), we obtained a comparatively high level of expression for plant-based expression systems in general (up to 120 mg per kg of fresh leaf material). Furthermore, we were able to eliminate the aggregates and recover the functional portion of rAH after extraction. Consequently, we have successfully developed a novel rAH expression platform that may be able to meet the manufacturing requirements for the protein to be developed as a topical HIV-1 microbicide.

Compared to other lectins that have been reported to exhibit anti-HIV-1 effects (reviewed in (7)), AH's antiviral activity reported here is not the strongest in this class. Notwithstanding the moderate anti-HIV-1 efficacy, AH's apparent lack of mitogenicity and cytotoxicity in hPBMCs demonstrated here is a clear advantage of this protein over some of the other anti-HIV-1 lectins. Using rDNA technology, it may be possible to engineer rAH derivatives that have stronger anti-HIV activity while maintaining quiescence in the toxicological aspects. In fact, in our preliminary

study, a recombinantly engineered AH dimer construct was shown to exhibit significantly stronger and broader anti-HIV-1 activity than the original monomer molecule (Tanaka & Matoba, manuscript in preparation). Based on the speed and robustness, the TMV-based rAH expression system will further facilitate the design of additional rAH analogues that have even more potent anti-HIV-1 activity and other desirable properties for microbicide use (e.g., producibility, bioavailability, formulability, etc.). Taken together, although further optimization is required, the TMV-based system may provide a viable means for the economical large-scale production as well as the design of rAH derivatives, which both significantly facilitate the development of rAH-based microbicide candidates.

In summary, we have demonstrated that: 1) AH exerts nanomolar-level antiviral activity against many clinically relevant HIV-1 strains of different clades and diverse cellular tropisms (with a possible exception for R5-type A clade viruses); 2) AH does not possess cytotoxicity or mitogenic activity in human PBMCs at doses showing broad anti-HIV activity; and 3) the TMV-based system serves as a novel rAH expression platform that may facilitate molecular engineering and economical large-scale production. Based on these initial efficacy, safety, and producibility data, we propose that AH is promising as a precursor of new candidate HIV-1 microbicides targeting Env glycans. Further investigation on efficacy and safety, analysis of mechanisms of action, and design of potent analogues are warranted.

Acknowledgments

The authors would like to thank Hillary Conway for her help in plant expression, Angela Freels for maintaining *N. benthamiana*, and Andrew Marsh for editorial assistance. The authors are grateful to Dr. Kenneth Palmer at University of Louisville School of Medicine for his

suggestions and critical reading of the manuscript. The work was supported in part by Owensboro Cancer Research Program startup funds (to N.M.) and an NIH Grant AI30034 to (D.C.M.). The magnICON TMV vector system was provided from Icon Genetics GmbH, Halle/Saale, Germany.

Conflict of interest: H.T. and K.T. are members of KIIM Pharmaceutical Laboratories, Inc., which owns the intellectual properties and the commercialization rights of AH. H.T., S.O. K.T., and A.T. are listed as inventors on patent applications related to AH.

Table 1. Anti-HIV-1 activity of AH against Env-pseudotyped viruses in TZM-bl cells.

Virus	Subtype	Genbank Accession No.	Tropism	IC_{50} (μg/ml)*	
				2G12	AH
MN.3	B	AY669737.1	X4	ND	0.04
SF162.LS	B	EU123924.1	R5	0.7	>25
W61D 7.12	B	AY973156.1	R5/X4	ND	9.9
Bal.26	B	DQ318211.1	R5	0.9	1.5
SS1196.1	B	AY835442.1	R5	10.8	0.01
Bx08.16	B	GQ855765.1	R5	5.4	2.3
BZ167.12	B	GQ855764.1	R5/X4	ND	2.9
6535.3	B	AY835438.1	R5	2	>25
QH0692.42	B	AY835439.1	R5	2.8	13.8
TRO.11	B	AY835445.1	R5	0.4	6.7
RHPA.7	B	AY835447.1	R5	>50	15.1
TV1.21	C	AF391231.1	R5	1.7	0.3
92BR025.9	C	U15121.1	R5	1.2	1.8
MW965.26	C	U08455.1	R5	>25	2.5
ZM214M.PL15	C	DQ388516.1	R5	>50	21.2
ZM109F.PB4	C	AY424138.2	R5	>50	>25
Q461.e2	A	AF407156.1	R5	>50	>25
Q259.d2.17	A	AF407152.1	R5	>50	>25
Q842.d12	A	AF407160.1	R5	>50	>25
Q168.a2	A	AF407148.1	R5	>50	>25

* IC_{50}s exceeding the highest concentrations of samples tested in the assay are shaded and expressed as >25 or >50 μg/ml.

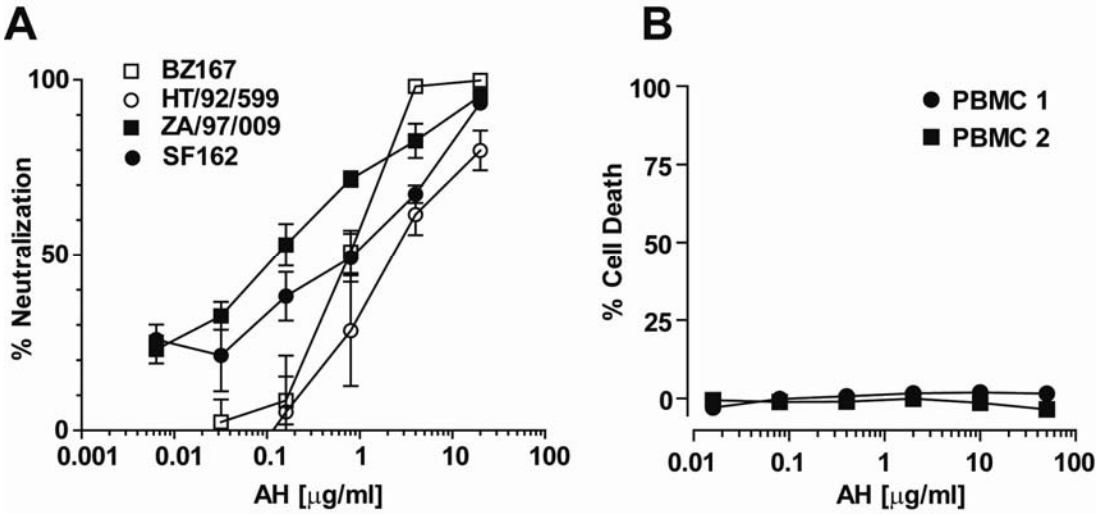

Figure 1. Neutralization of primary HIV-1 isolates in human PBMCs. (A) The PBMC-based neutralization assay. The reduction of p24 gag protein production in human PBMCs was measured as an endpoint. PBMCs (pooled from four different donors) were infected with R5 B clade (SF162), R5 C clade (ZA/97/009), X4 B clade (HT/92/599), or R5X4 B clade (BZ167) in the presence of various concentrations of AH. Samples were analyzed in quadruplicate. Results are expressed as mean ± SEM. See Materials and Methods for assay details. Dose-dependent neutralization was observed for all viruses. (B) Cytotoxicity analysis. Potential toxicity of AH in human PBMCs was analyzed based on the LDH activity in the culture medium after incubation of PBMCs with various concentrations of AH. Analysis was performed in quadruplicate in two different pools of human PBMCs. Results are expressed as mean ± SEM. The lack of PMBC cytotoxicity was demonstrated for up to 50 μg/ml of AH.

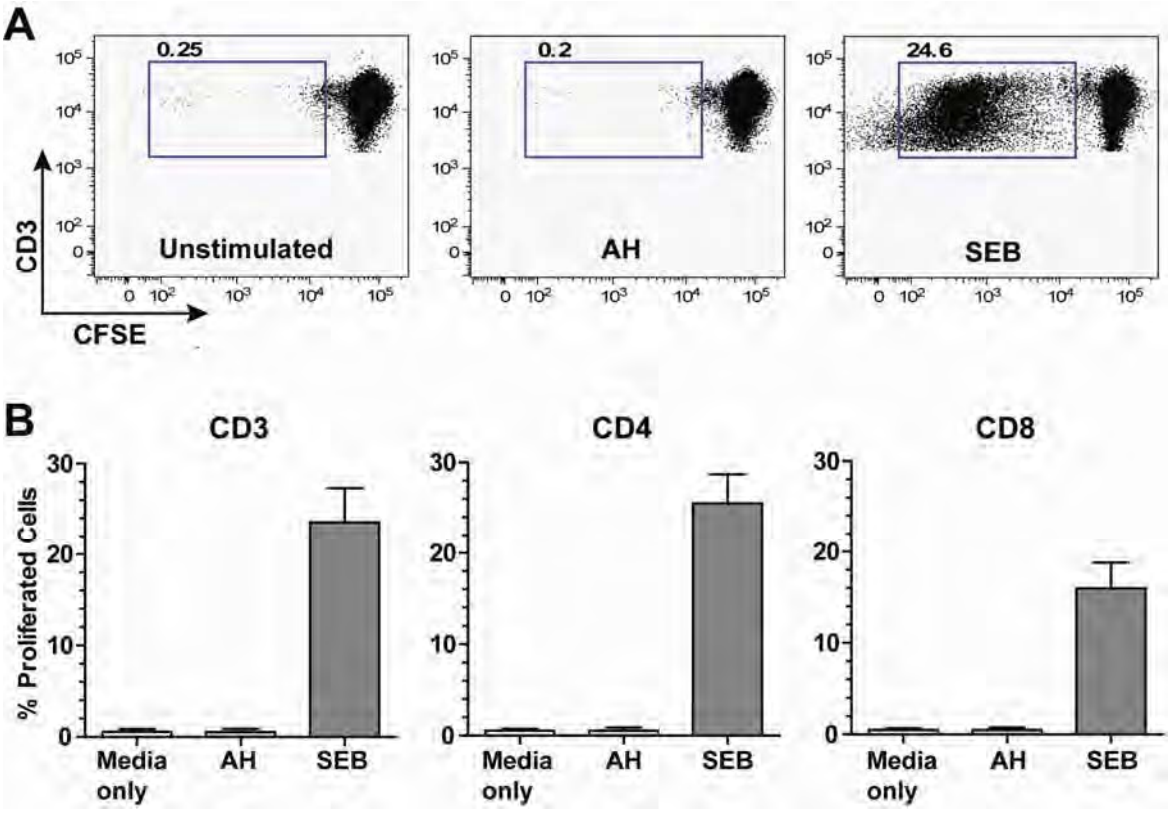

519

520 **Figure 2. Analysis of mitogenic activity in human PBMCs.** Proliferation of human $CD3^+$
521 lymphocytes in PBMCs was analyzed by flow cytometry. CFSE-stained human PBMCs were
522 incubated for 5 days with 12.5 μg/ml AH, 1 μg/ml SEB (positive control; a potent T cell
523 stimulator (21, 57)), or media alone. Samples were first gated on a viable T cell population, and
524 the percentage of proliferating cells was determined based on the extent of CFSE dilution. (A)
525 Representative plots from one of three experiments are shown for $CD3^+$ cells. The number in
526 each panel (above the boxed plot population) indicates the percentage of proliferated cells. (B)
527 Results from 3 independent experiments using different PBMCs are shown. In addition to $CD3^+$
528 cells, $CD4^+$ and $CD8^+$ cells were analyzed to further dissect proliferative potential. Results are
529 expressed as mean ± SD. AH did not show any mitogenic activity in any cell types tested.

530

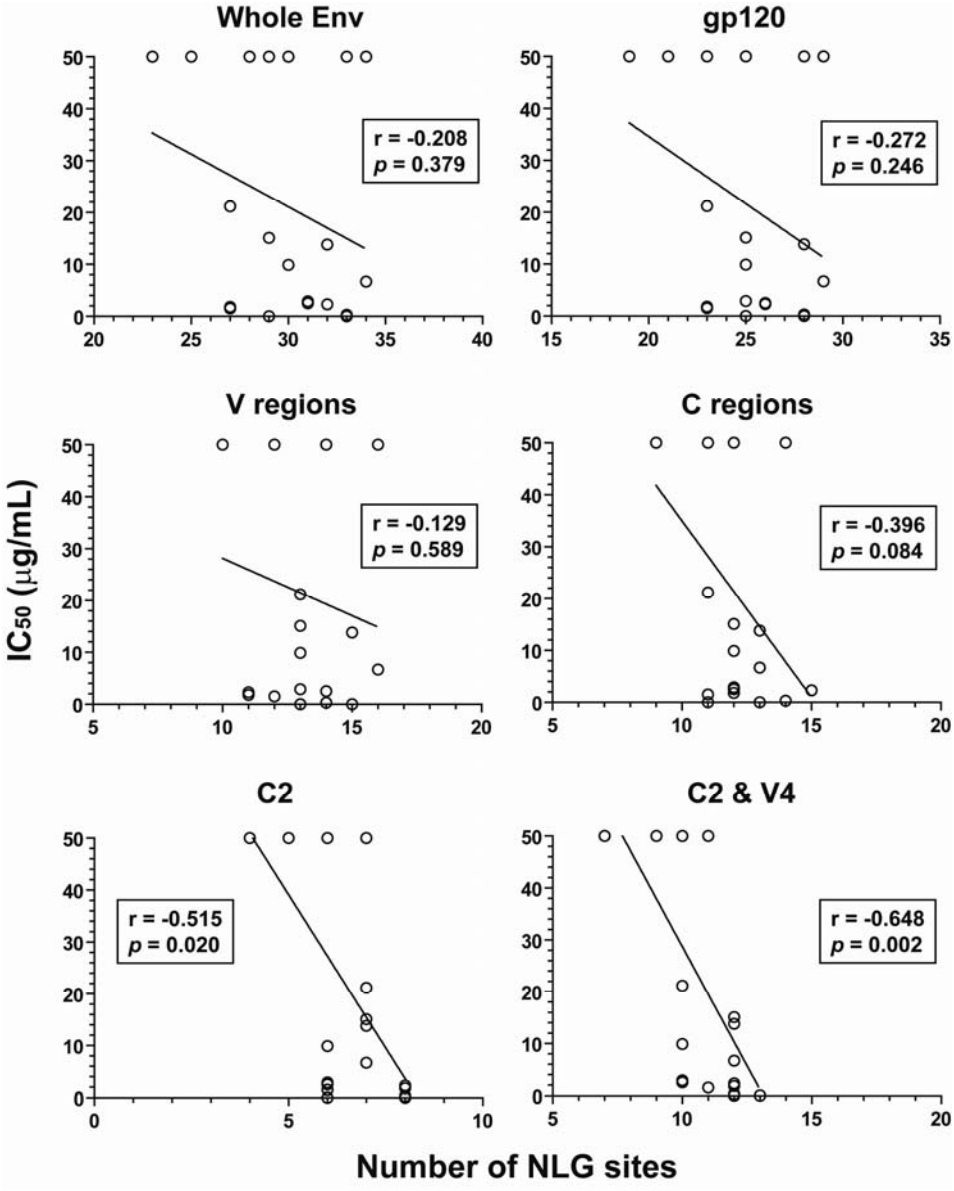

Figure 3. Correlation between the number of NLG sequons and AH susceptibility in Env-pseudotyped viruses. For each virus tested in the TZM-bl-based assay, the number of NLG sites (i.e., sequons) in the indicated Env region was plotted against the IC_{50}. The IC_{50} values of >25 μg/ml were approximated to 50 μg/ml. Correlation was analyzed by the non-parametric Spearman's correlation coefficient. The correlation coefficient (r) and *p* values are shown in the box in each graph. A *p* value of less than 0.05 is regarded as statistically significant. Linear regression analysis was used to display a best fit line to the data.

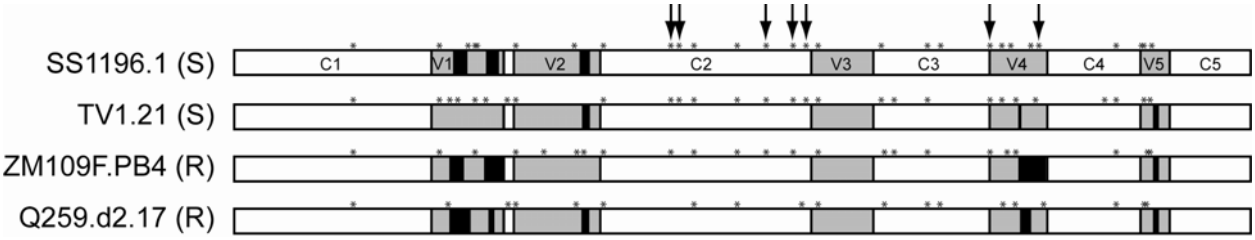

Figure 4. Schematic representation of Env and potential NLG positions in selected AH-susceptible and -resistant viruses. Constant regions (C1 – C5; shown in white) and variable regions (V1 – V5; shown in grey) are shown for the two most susceptible viruses (SS1196.1 and TV1.21) and two highly resistant viruses (ZM109F.PB4 and Q259.d2.17) to AH, according to the results shown in Table 2. Black boxes indicate deletions in the corresponding regions. Asterisks represent the position of sequons. Potential targets of AH within the C2 and V4 regions (those present in both the susceptible viruses but absent in either of the resistant strains) are indicated by arrows.

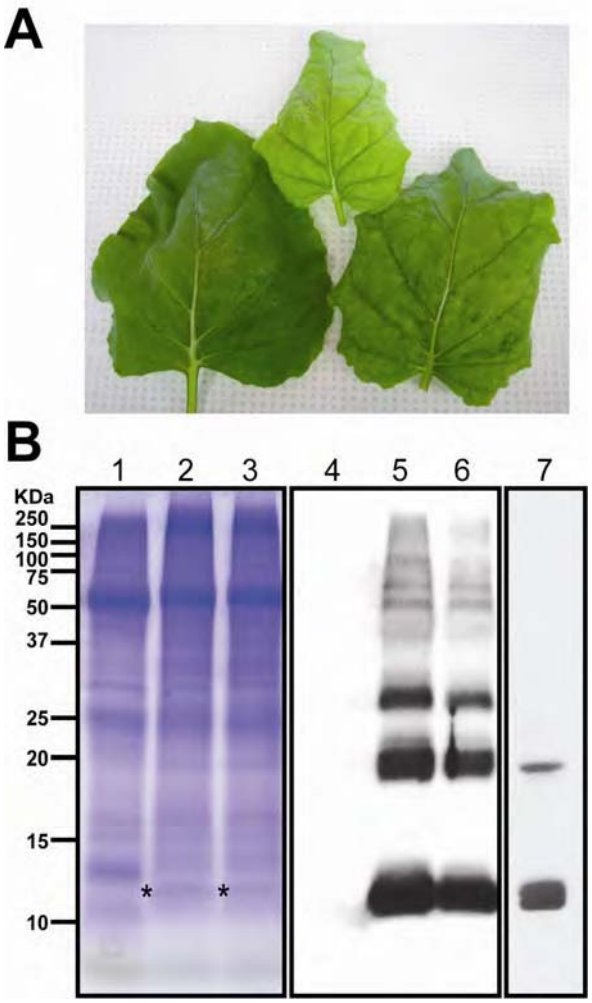

Figure 5. Expression of rAH in *N. benthamiana*. (A) Representative TMV vector-infiltrated *N. benthamiana* leaves at 6 dpi. The leaves show only a minor level of tissue necrosis. (B) Electrophoretic analysis of rAH expression in leaf extract. Coomassie-stained SDS-PAGE gel (Lanes 1 – 3) and western blot analysis (Lanes 4 – 7) are shown. Total leaf proteins were extracted in a buffer containing 2% SDS and separated under reducing conditions. Lanes 1 and 4: non-infiltrated control leaf extract; lanes 2, 3, 5, and 6: vector-infiltrated leaf extracts made from two independent infiltration events; and lane 7: the dialyzed aqueous fraction of infiltrated leaf proteins prepared by 6M guanidine buffer extraction. Asterisks indicate the bands corresponding to rAH (Mw: 12.5 kDa). Efficient extraction of gp120-binding rAH required a buffer containing a chaotropic agent such as SDS or guanidine HCl. The fraction contains apparent multimers of rAH (Lanes 5 and 6). These aggregates are largely absent after dialysis, while the monomer protein stays soluble (Lane 7). See text for detail.

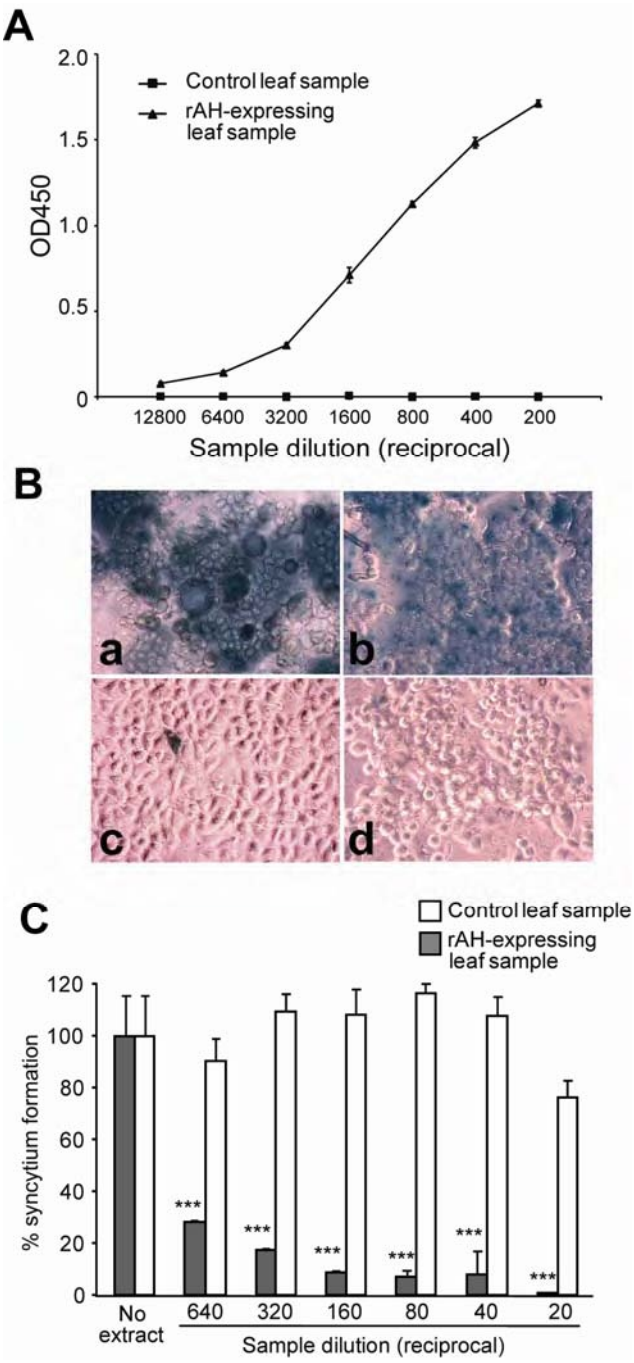

Figure 6. Activity analysis of *N. benthamiana*-expressed rAH. (A) The gp120-binding capacity of rAH expressed in *N. benthamiana* was evaluated by gp120-ELISA using AH-expressing and control (uninfilatrated) leaf extracts prepared as described in Materials and Methods. Results of a representative sample obtained from a ~2 g batch of leaf materials are shown. Data points are the means ± SD of triplicate analysis. This analysis was also used to determine the quantity of rAH in the extract based on a standard curve created by actinomycete-derived purified AH. (B) X-gal staining of syncytia formation by HeLa/Env/tat and HeLa/CD4/LacZ. The two cell lines were incubated for 18 h at 37°C with: **a**, media alone; **b**, 1/20-diluted non-infiltrated control leaf sample; **c**, 1 μM actinomycete-derived AH; and **d**, 1/20-diluted rAH-expressing leaf sample (containing approximately 0.32 μM, or 4.0 μg/ml, of rAH, as determined by gp120-ELISA). (C) Quantitative analysis of syncytia formation by HeLa/Env/tat and HeLa/CD4/LacZ. The two cell lines were incubated for 18 h at 37°C with serially diluted control or rAH-expressing leaf samples. See Materials and Methods for the assay detail. Differences between the samples at each dilution point were evaluated by two-way analysis of variance followed by Bonferroni posttests (*** $p < 0.001$).

References

1. AIDS epidemic update (2009) AIDS epidemic update., Joint United Nations Programme on HIV/AIDS & World Health Organization
2. Garg, A. B., Nuttall, J., and Romano, J. (2009) The future of HIV microbicides: challenges and opportunities. *Antivir Chem Chemother* 19, 143-150
3. McGowan, I. (2010) Microbicides for HIV prevention: reality or hope? *Curr Opin Infect Dis* 23, 26-31
4. Morris, G. C., and Lacey, C. J. (2010) Microbicides and HIV prevention: lessons from the past, looking to the future. *Curr Opin Infect Dis* 23, 57-63
5. Grant, R. M., Hamer, D., Hope, T., Johnston, R., Lange, J., Lederman, M. M., Lieberman, J., Miller, C. J., Moore, J. P., Mosier, D. E., Richman, D. D., Schooley, R. T., Springer, M. S., Veazey, R. S., and Wainberg, M. A. (2008) Whither or wither microbicides? *Science* 321, 532-534
6. Scanlan, C. N., Offer, J., Zitzmann, N., and Dwek, R. A. (2007) Exploiting the defensive sugars of HIV-1 for drug and vaccine design. *Nature* 446, 1038-1045
7. Balzarini, J. (2007) Targeting the glycans of glycoproteins: a novel paradigm for antiviral therapy. *Nature reviews* 5, 583-597
8. Swanson, M. D., Winter, H. C., Goldstein, I. J., and Markovitz, D. M. (2010) A lectin isolated from bananas is a potent inhibitor of HIV replication. *J Biol Chem*
9. Calarese, D. A., Lee, H. K., Huang, C. Y., Best, M. D., Astronomo, R. D., Stanfield, R. L., Katinger, H., Burton, D. R., Wong, C. H., and Wilson, I. A. (2005) Dissection of the carbohydrate specificity of the broadly neutralizing anti-HIV-1 antibody 2G12. *Proc Natl Acad Sci U S A* 102, 13372-13377

10. Scanlan, C. N., Pantophlet, R., Wormald, M. R., Ollmann Saphire, E., Stanfield, R., Wilson, I. A., Katinger, H., Dwek, R. A., Rudd, P. M., and Burton, D. R. (2002) The broadly neutralizing anti-human immunodeficiency virus type 1 antibody 2G12 recognizes a cluster of alpha1-->2 mannose residues on the outer face of gp120. *J Virol* 76, 7306-7321

11. Chiba, H., Inokoshi, J., Okamoto, M., Asanuma, S., Matsuzaki, K., Iwama, M., Mizumoto, K., Tanaka, H., Oheda, M., Fujita, K., Nakashima, H., Shinose, M., Takahashi, Y., and Omura, S. (2001) Actinohivin, a novel anti-HIV protein from an actinomycete that inhibits syncytium formation: isolation, characterization, and biological activities. *Biochem Biophys Res Commun* 282, 595-601

12. Takahashi, A., Inokoshi, J., Chiba, H., Omura, S., and Tanaka, H. (2005) Essential regions for antiviral activities of actinohivin, a sugar-binding anti-human immunodeficiency virus protein from an actinomycete. *Arch Biochem Biophys* 437, 233-240

13. Tanaka, H., Chiba, H., Inokoshi, J., Kuno, A., Sugai, T., Takahashi, A., Ito, Y., Tsunoda, M., Suzuki, K., Sekiguchi, T., Takenaka, A., Umeyama, H., Hirabayashi, J., and Omura, S. (2009) Mechanism by which the lectin actinohivin blocks HIV infection of target cells. *Proc Natl Acad Sci U S A* 106, 15633-15638

14. Lin, G., Simmons, G., Pohlmann, S., Baribaud, F., Ni, H., Leslie, G. J., Haggarty, B. S., Bates, P., Weissman, D., Hoxie, J. A., and Doms, R. W. (2003) Differential N-linked glycosylation of human immunodeficiency virus and Ebola virus envelope glycoproteins modulates interactions with DC-SIGN and DC-SIGNR. *J Virol* 77, 1337-1346

15. Chiba, H., Inokoshi, J., Nakashima, H., Omura, S., and Tanaka, H. (2004) Actinohivin, a novel anti-human immunodeficiency virus protein from an actinomycete, inhibits viral entry to cells by binding high-mannose type sugar chains of gp120. *Biochem Biophys Res Commun* 316, 203-210

16. Fenyo, E. M., Heath, A., Dispinseri, S., Holmes, H., Lusso, P., Zolla-Pazner, S., Donners, H., Heyndrickx, L., Alcami, J., Bongertz, V., Jassoy, C., Malnati, M., Montefiori, D., Moog, C., Morris, L., Osmanov, S., Polonis, V., Sattentau, Q., Schuitemaker, H., Sutthent, R., Wrin, T., and Scarlatti, G. (2009) International network for comparison of HIV neutralization assays: the NeutNet report. *PLoS ONE* 4, e4505

17. D'Souza, M. P., Milman, G., Bradac, J. A., McPhee, D., Hanson, C. V., and Hendry, R. M. (1995) Neutralization of primary HIV-1 isolates by anti-envelope monoclonal antibodies. *Aids* 9, 867-874

18. Mascola, J. R., Louder, M. K., Surman, S. R., Vancott, T. C., Yu, X. F., Bradac, J., Porter, K. R., Nelson, K. E., Girard, M., McNeil, J. G., McCutchan, F. E., Birx, D. L., and Burke, D. S. (1996) Human immunodeficiency virus type 1 neutralizing antibody serotyping using serum pools and an infectivity reduction assay. *AIDS Res Hum Retroviruses* 12, 1319-1328

19. Wang, C. Y., Sawyer, L. S., Murthy, K. K., Fang, X., Walfield, A. M., Ye, J., Wang, J. J., Chen, P. D., Li, M. L., Salas, M. T., Shen, M., Gauduin, M. C., Boyle, R. W., Koup, R. A., Montefiori, D. C., Mascola, J. R., Koff, W. C., and Hanson, C. V. (1999) Postexposure immunoprophylaxis of primary isolates by an antibody to HIV receptor complex. *Proc Natl Acad Sci U S A* 96, 10367-10372

20. Elrefaei, M., McElroy, M. D., Preas, C. P., Hoh, R., Deeks, S., Martin, J., and Cao, H. (2004) Central memory CD4+ T cell responses in chronic HIV infection are not restored by antiretroviral therapy. *J Immunol* 173, 2184-2189

21. Fraser, J. D., and Proft, T. (2008) The bacterial superantigen and superantigen-like proteins. *Immunol Rev* 225, 226-243

22. Montefiori, D. C. (2009) Measuring HIV neutralization in a luciferase reporter gene assay. *Methods Mol Biol* 485, 395-405

671 23. Zhang, M., Gaschen, B., Blay, W., Foley, B., Haigwood, N., Kuiken, C., and Korber, B.
672 (2004) Tracking global patterns of N-linked glycosylation site variation in highly variable
673 viral glycoproteins: HIV, SIV, and HCV envelopes and influenza hemagglutinin.
674 *Glycobiology* 14, 1229-1246
675 24. Marillonnet, S., Giritch, A., Gils, M., Kandzia, R., Klimyuk, V., and Gleba, Y. (2004) In
676 planta engineering of viral RNA replicons: efficient assembly by recombination of DNA
677 modules delivered by Agrobacterium. *Proc Natl Acad Sci U S A* 101, 6852-6857
678 25. Marillonnet, S., Thoeringer, C., Kandzia, R., Klimyuk, V., and Gleba, Y. (2005) Systemic
679 Agrobacterium tumefaciens-mediated transfection of viral replicons for efficient transient
680 expression in plants. *Nat Biotechnol* 23, 718-723
681 26. Chiba, H., Asanuma, S., Okamoto, M., Inokoshi, J., Tanaka, H., Fujita, K., and Omura, S.
682 (2001) A simple screening system for anti-HIV drugs: syncytium formation assay using
683 T-cell line tropic and macrophage tropic HIV env expressing cell lines--establishment
684 and validation. *J Antibiot (Tokyo)* 54, 818-826
685 27. Sharon, N., and Lis, H. (2004) History of lectins: from hemagglutinins to biological
686 recognition molecules. *Glycobiology* 14, 53R-62R
687 28. Gavrovic-Jankulovic, M., Poulsen, K., Brckalo, T., Bobic, S., Lindner, B., and Petersen,
688 A. (2008) A novel recombinantly produced banana lectin isoform is a valuable tool for
689 glycoproteomics and a potent modulator of the proliferation response in CD3+, CD4+,
690 and CD8+ populations of human PBMCs. *Int J Biochem Cell Biol* 40, 929-941
691 29. Huskens, D., Vermeire, K., Vandemeulebroucke, E., Balzarini, J., and Schols, D. (2008)
692 Safety concerns for the potential use of cyanovirin-N as a microbicidal anti-HIV agent. *Int*
693 *J Biochem Cell Biol* 40, 2802-2814
694 30. Balzarini, J., Van Laethem, K., Peumans, W. J., Van Damme, E. J., Bolmstedt, A., Gago,
695 F., and Schols, D. (2006) Mutational pathways, resistance profile, and side effects of

cyanovirin relative to human immunodeficiency virus type 1 strains with N-glycan deletions in their gp120 envelopes. *J Virol* 80, 8411-8421

31. Lederman, M. M., Jump, R., Pilch-Cooper, H. A., Root, M., and Sieg, S. F. (2008) Topical application of entry inhibitors as "virustats" to prevent sexual transmission of HIV infection. *Retrovirology* 5, 116

32. Pope, M., and Haase, A. T. (2003) Transmission, acute HIV-1 infection and the quest for strategies to prevent infection. *Nat Med* 9, 847-852

33. Taylor, B. S., Sobieszczyk, M. E., McCutchan, F. E., and Hammer, S. M. (2008) The challenge of HIV-1 subtype diversity. *N Engl J Med* 358, 1590-1602

34. Buonaguro, L., Tornesello, M. L., and Buonaguro, F. M. (2007) Human immunodeficiency virus type 1 subtype distribution in the worldwide epidemic: pathogenetic and therapeutic implications. *J Virol* 81, 10209-10219

35. Calarese, D. A., Scanlan, C. N., Zwick, M. B., Deechongkit, S., Mimura, Y., Kunert, R., Zhu, P., Wormald, M. R., Stanfield, R. L., Roux, K. H., Kelly, J. W., Rudd, P. M., Dwek, R. A., Katinger, H., Burton, D. R., and Wilson, I. A. (2003) Antibody domain exchange is an immunological solution to carbohydrate cluster recognition. *Science* 300, 2065-2071

36. Inokoshi, J., Chiba, H., Asanuma, S., Takahashi, A., Omura, S., and Tanaka, H. (2001) Molecular cloning of actinohivin, a novel anti-HIV protein from an actinomycete, and its expression in Escherichia coli. *Biochem Biophys Res Commun* 281, 1261-1265

37. Polonis, V. R., Brown, B. K., Rosa Borges, A., Zolla-Pazner, S., Dimitrov, D. S., Zhang, M. Y., Barnett, S. W., Ruprecht, R. M., Scarlatti, G., Fenyo, E. M., Montefiori, D. C., McCutchan, F. E., and Michael, N. L. (2008) Recent advances in the characterization of HIV-1 neutralization assays for standardized evaluation of the antibody response to infection and vaccination. *Virology* 375, 315-320

38. Keller, M. J., and Herold, B. C. (2009) Understanding basic mechanisms and optimizing assays to evaluate the efficacy of vaginal microbicides. *Sex Transm Dis* 36, S92-95

722 39. Willey, R. L., Shibata, R., Freed, E. O., Cho, M. W., and Martin, M. A. (1996) Differential
723 glycosylation, virion incorporation, and sensitivity to neutralizing antibodies of human
724 immunodeficiency virus type 1 envelope produced from infected primary T-lymphocyte
725 and macrophage cultures. *J Virol* 70, 6431-6436
726 40. Liedtke, S., Geyer, R., and Geyer, H. (1997) Host-cell-specific glycosylation of HIV-2
727 envelope glycoprotein. *Glycoconj J* 14, 785-793
728 41. Yuste, E., Reeves, J. D., Doms, R. W., and Desrosiers, R. C. (2004) Modulation of Env
729 content in virions of simian immunodeficiency virus: correlation with cell surface
730 expression and virion infectivity. *J Virol* 78, 6775-6785
731 42. Bachrach, E., Dreja, H., Lin, Y. L., Mettling, C., Pinet, V., Corbeau, P., and Piechaczyk,
732 M. (2005) Effects of virion surface gp120 density on infection by HIV-1 and viral
733 production by infected cells. *Virology* 332, 418-429
734 43. Peters, P. J., Sullivan, W. M., Duenas-Decamp, M. J., Bhattacharya, J., Ankghuambom,
735 C., Brown, R., Luzuriaga, K., Bell, J., Simmonds, P., Ball, J., and Clapham, P. R. (2006)
736 Non-macrophage-tropic human immunodeficiency virus type 1 R5 envelopes
737 predominate in blood, lymph nodes, and semen: implications for transmission and
738 pathogenesis. *J Virol* 80, 6324-6332
739 44. Paranjpe, S., Craigo, J., Patterson, B., Ding, M., Barroso, P., Harrison, L., Montelaro, R.,
740 and Gupta, P. (2002) Subcompartmentalization of HIV-1 quasispecies between seminal
741 cells and seminal plasma indicates their origin in distinct genital tissues. *AIDS Res Hum*
742 *Retroviruses* 18, 1271-1280
743 45. O'Keefe, B. R., Vojdani, F., Buffa, V., Shattock, R. J., Montefiori, D. C., Bakke, J.,
744 Mirsalis, J., d'Andrea, A. L., Hume, S. D., Bratcher, B., Saucedo, C. J., McMahon, J. B.,
745 Pogue, G. P., and Palmer, K. E. (2009) Scaleable manufacture of HIV-1 entry inhibitor
746 griffithsin and validation of its safety and efficacy as a topical microbicide component.
747 *Proc Natl Acad Sci U S A*

46. Zhu, X., Borchers, C., Bienstock, R. J., and Tomer, K. B. (2000) Mass spectrometric characterization of the glycosylation pattern of HIV-gp120 expressed in CHO cells. *Biochemistry* 39, 11194-11204

47. Leonard, C. K., Spellman, M. W., Riddle, L., Harris, R. J., Thomas, J. N., and Gregory, T. J. (1990) Assignment of intrachain disulfide bonds and characterization of potential glycosylation sites of the type 1 recombinant human immunodeficiency virus envelope glycoprotein (gp120) expressed in Chinese hamster ovary cells. *J Biol Chem* 265, 10373-10382

48. Cutalo, J. M., Deterding, L. J., and Tomer, K. B. (2004) Characterization of glycopeptides from HIV-I(SF2) gp120 by liquid chromatography mass spectrometry. *J Am Soc Mass Spectrom* 15, 1545-1555

49. Shenoy, S. R., Barrientos, L. G., Ratner, D. M., O'Keefe, B. R., Seeberger, P. H., Gronenborn, A. M., and Boyd, M. R. (2002) Multisite and multivalent binding between cyanovirin-N and branched oligomannosides: calorimetric and NMR characterization. *Chem Biol* 9, 1109-1118

50. Botos, I., O'Keefe, B. R., Shenoy, S. R., Cartner, L. K., Ratner, D. M., Seeberger, P. H., Boyd, M. R., and Wlodawer, A. (2002) Structures of the complexes of a potent anti-HIV protein cyanovirin-N and high mannose oligosaccharides. *J Biol Chem* 277, 34336-34342

51. Tsai, C. C., Emau, P., Jiang, Y., Tian, B., Morton, W. R., Gustafson, K. R., and Boyd, M. R. (2003) Cyanovirin-N gel as a topical microbicide prevents rectal transmission of SHIV89.6P in macaques. *AIDS Res Hum Retroviruses* 19, 535-541

52. Tsai, C. C., Emau, P., Jiang, Y., Agy, M. B., Shattock, R. J., Schmidt, A., Morton, W. R., Gustafson, K. R., and Boyd, M. R. (2004) Cyanovirin-N inhibits AIDS virus infections in vaginal transmission models. *AIDS Res Hum Retroviruses* 20, 11-18

53. Buffa, V., Stieh, D., Mamhood, N., Hu, Q., Fletcher, P., and Shattock, R. J. (2009) Cyanovirin-N potently inhibits human immunodeficiency virus type 1 infection in cellular and cervical explant models. *J Gen Virol* 90, 234-243

54. Zeitlin, L., Pauly, M., and Whaley, K. J. (2009) Second-generation HIV microbicides: continued development of griffithsin. *Proc Natl Acad Sci U S A* 106, 6029-6030

55. Ma, J. K., Chikwamba, R., Sparrow, P., Fischer, R., Mahoney, R., and Twyman, R. M. (2005) Plant-derived pharmaceuticals--the road forward. *Trends Plant Sci* 10, 580-585

56. Matoba, N., Davis, K. R., and Palmer, K. E. (in press) Recombinant Protein Expression in Nicotiana. *Methods Mol Biol*

57. Alouf, J. E., and Muller-Alouf, H. (2003) Staphylococcal and streptococcal superantigens: molecular, biological and clinical aspects. *Int J Med Microbiol* 292, 429-440